Infrared Laser-Induced Photolysis of Ethylene

by

Ronald J. Corkum, B.Sc.

A thesis submitted in partial fulfilment

of the requirements for the degree of

Master of Science

in the

Department of Chemistry

University of Ottawa

Ottawa, Canada

1978

Margaret H. Back

Margaret H. Back,
Professor of Chemistry,
Research Supervisor

Ronald Corkum

Ronald Corkum,
M.Sc. Candidate

Acknowledgements

I wish to express appreciation to my supervisor, Dr. Margaret Back, for her guidance and encouragement throughout the performance of this work. I am grateful to everyone in the Photochemistry Section with whom I have had the pleasure of working during my stay at N.R.C. I would particularly like to thank Drs. Robert Back and Clive Willis for many helpful discussions. I am indebted to John Parsons and Roger Pilon for their willing assistance with experimental work. Finally, I would like to thank my parents for their constant support.

Abstract

The decomposition of ethylene by high-power infrared laser radiation has been studied. The influence of pressure, beam intensity, and irradiation time on the product distribution was investigated. Isotopic mixtures were also irradiated to gain insight into the mechanism and to investigate isotopic selectivity of the process.

Changes in mechanism were apparent as the reactant pressure was varied. Evidence is present for a low pressure, collisionless, isotopically-selective multiphoton process. At higher pressures, collisions produce relaxation of vibrational energy and a diffusion-controlled thermal pyrolysis becomes the important process. There is a pressure threshold for a given intensity above which optical breakdown occurs accompanied by visible luminescence and rapid decomposition.

Table of Contents

Chapter One: Introduction

I. Lasers and Properties of Laser Radiation

The development of the laser has been of great importance to modern scientific research. This is due to the special properties of laser radiation[1]. The output from a laser is brought about by stimulated emission corresponding to an electronic or vibrational transition from excited atoms or molecules. A population inversion must exist for which the upper state is more populated than the lower level. This may be achieved by electrical or microwave discharge, electron beams, ultraviolet flashlamps, chemical reactions, or with the use of another laser. The lasing action is initiated by spontaneous emission from some of the excited species which induces a cascade of spatially coherent stimulated emission. High intensity and extremely narrow frequency width is possible as a result of amplification which occurs by multiple passes of the light between the reflecting surfaces of the laser cavity. The gain characteristics of the laser sharpen the spectral distribution of the stimulated emission because the peak frequency is preferentially enhanced.

Lasers may be either continuous wave (CW) or pulsed. The output from a continuous wave laser is in the form of an uninterrupted beam of steady intensity. Pulsed lasers emit periodic bursts of energy which can be of extremely high intensity at the peak of the pulse. Pulse durations vary from shorter than one picosecond to several hundred microseconds.

The ability to vary the frequency of radiation is known as tunability. The output of line-tunable lasers is restricted to a set of discrete frequencies; continuously tunable lasers allow selection of any desired frequency over the spectral range of the output[2].

A wide variety of materials has been observed to lase in a frequency range extending from the far infrared to the vacuum ultraviolet regions of the spectrum. Solid state lasers use ions doped in a transparent host crystal as the active medium. Common examples are the ruby laser (chromium ions in sapphire) and Nd-YAG laser (neodymium ions in yttrium aluminum garnet). Gas lasers may be neutral atomic (e.g. helium-neon), ionic (e.g. cadmium, argon, krypton), or molecular (e.g. CO_2, HF, N_2). Compact semiconductor diode lasers have been developed (e.g. Ga-As, Pb-Sn-Te) which directly convert electrical energy into laser radiation of very narrow spectral width. Tunable dye lasers use organic dyes as lasing material which fluoresce over a wide range of wavelengths in the visible spectrum. Tunable ultraviolet radiation can be obtained by the frequency doubling technique whereby visible radiation inside the laser cavity is doubled in frequency as it passes through a crystal with non-linear properties. Ultraviolet radiation is also available from the newly developed excimer laser where lasing occurs from a rare gas-halide complex stable only in the excited state.

II. Lasers in Chemistry

Lasers have been important as research tools in many branches of chemistry. The high intensity and narrow frequency width of laser radiation has allowed spectroscopists to obtain greater resolution than ever before possible. In addition to atoms and molecules, the spectra of free radicals and ions are being studied using laser spectroscopy. The field of Raman spectroscopy has been revolutionized with the advent of lasers.

Molecular dynamicists have utilized laser techniques for monitoring changes in energy states during physical or chemical processes. Subnanosecond pulsed lasers have been used as probes to study the kinetics of fast processes.

Analytical chemists have adopted lasers for a variety of uses. Laser-excited atomic fluorescence flame spectrometry, laser intracavity absorption spectrometry, and laser microprobe chemical analysis are examples of newly developed analytical techniques. Remote sensing of atmospheric pollutants by detecting absorption, emission, or scattering of laser light by molecules is another recent development.

Of particular interest to many chemists is the field of laser-induced chemical reactions. It is known that photochemical reactions often follow different pathways than thermal reactions. Photochemical reactions have generally been induced by exciting electronic transitions of reactants using visible and ultraviolet radiation produced from gas discharge lamps. Laser radiation is superior to the broadband output of an arc or flashlamp because of its high intensity and narrow spectral

distribution. Visible and frequency-doubled ultraviolet lasers have been employed in a number of recent photochemical studies. Since laser sources have not been extensively developed in the ultraviolet, research in this region has been hindered. However, recent efforts in laser technology hold promise in providing photochemists with efficient ultraviolet laser sources[3].

An intriguing aspect of laser-induced photochemistry is the separation of isotopic species. The method is based upon the fact that atoms or molecules of different isotopic composition absorb light at different wavelengths so that one isotope in a mixture can be selectively activated. The very intense, monochromatic radiation obtainable from a laser is ideally suited for this purpose. Many isotope separation techniques have been developed using a variety of lasers to excite the desired isotopic species. Subsequent physical or chemical processes are employed to complete the separation. The separation of the excited species must be rapid to avoid randomization of the absorbed energy through collisional exchange. Hundreds of isotope separations have already been reported in the literature. This area has great potential usefulness for applications in industry and basic research. The subject is reviewed in references 4, 5, and 6.

III. Infrared Laser-Induced Reactions

Infrared laser-induced chemical reactions in the gas phase have been the subject of much attention in the past several years[6]. The mechanisms by which these reactions proceed depend on a number of variables.

Reaction may be induced by simple heating in which case the energy initially absorbed is randomized by collisional transfer among the gas molecules. High reactant pressure, long pulse duration or CW irradiation, and low peak intensity favor thermalization of absorbed laser energy. These conditions can be advantageous when a homogeneous thermal reaction is desired. A laser-induced thermolysis can avoid side reactions catalyzed on the walls of the reaction vessel which often occur in conventional thermolysis techniques[7].

Reaction may also occur from reagents rich in vibrational energy before a Boltzmann distribution is achieved. Selective energy deposition in a mode leading to reaction may be much more effective in enhancing reaction rate than random energization produced by heating. Nonthermal bimolecular reactions have been enhanced using infrared lasers in a number of studies[8].

It is possible that exchange of vibrational energy (V-V transfer) through collisions of excited gas molecules can result in certain of the molecules ascending the vibrational manifold until they have acquired sufficient energy for dissociation or reaction. This "stepladder" or "cascade" process occurs under conditions of higher intensity, shorter pulse duration, and lower pressure than for a thermal pyrolysis mechanism.

Recently it has been found that under the influence of an intense infrared field, many polyatomic molecules can be excited to the state of dissociation even at pressures sufficiently

low that the time for the excitation process is shorter than the mean time between collisions. Since the energy of one infrared photon is much less than that required to dissociate a molecule it is apparent that many photons are being very rapidly absorbed. This phenomenon has been referred to as multiple photon or "multiphoton" absorption.

Infrared multiphoton absorption was first experimentally observed by Isenor and Richardson[9] in 1970. On irradiation of a number of gases with intense infrared light from a pulsed carbon dioxide TEA laser, they observed a fast fluorescence pulse from the irradiated gas occurring with no detectable time delay after the laser pulse. The fluorescence was found to be characteristic of breakdown products of the irradiated gas indicating that some of the molecules had been dissociated before collisional processes had set in.

The potential of the multiphoton collisionless decomposition process for selective separation of isotopic species was soon realized. In 1974 the two isotopes of boron were separated[10] by selective infrared irradiation of boron trichloride gas. The dissociated boron atoms of one isotope reacted with oxygen scavenger molecules leaving the remaining BCl_3 enriched in the unexcited isotope. Subsequently isotopes of sulfur, hydrogen, carbon, silicon, chlorine, selenium, and osmium have been enriched by multiphoton processes. (Reference 11 gives a number of examples).

It is interesting that the multiphoton mechanism enables a molecule to be excited up the vibrational ladder to

dissociation by the narrow frequency distribution of light from the laser which corresponds to the v=0 to v=1 transition of a vibrational mode. A decrease in energy spacing between successive levels of vibrational excitation occurs due to the anharmonic nature of the vibrations of a real molecule. One might expect that this "anharmonic defect" would cause the laser frequency to go out of resonance with higher transitions preventing high vibrational excitation and dissociation.

The fact that multiphoton irradiations are isotopically selective indicates that the resonance between laser and molecular vibrational frequencies is important. This suggests that the multiphoton process does not occur by simultaneous absorption of large numbers of photons. It appears to involve stepwise collisionless accumulation of vibrational energy at least in the initial stages of the process.

It is known that in an intense electric field, the energy levels of a molecule are split (Stark Effect) and broadened. The magnitude of the power broadening is proportional to the product of the electric field and the transition dipole moment. The electric field generated by infrared laser radiation can be sufficiently large that broadening of vibrational levels allows resonant absorption of several quanta of vibrational energy. Once a certain level of vibrational excitation has been reached it appears that the resonant characteristic of the laser frequency is no longer essential for further excitation. This situation arises since the normal coordinate approximation for vibrations in polyatomic molecules breaks down for high

levels of excitation. At this stage rapid intramolecular energy distribution can occur among the vibrational modes. Since a polyatomic molecule has many vibrational modes, the density of energy levels rises rapidly with increasing excitation until a certain threshold is attained where there is essentially a continuum of levels available. When this "quasicontinuum" of energy states has been reached subsequent absorption of laser radiation can occur up to the dissociation limit without wavelength specificity.

Recently this model has been tested[12] by an experiment using two infrared lasers at different frequencies to bring about decomposition of sulfur hexafluoride. The first laser of relatively weak intensity was tuned to be resonant with the $v=0$ to $v=1$ transition of the ν_3 mode of SF_6. The second laser was tuned far off resonance and was of high intensity. It was found that the intensities of both laser frequencies could be adjusted so that dissociation would only occur with both fields present. The interpretation was given that the first laser brought about resonant excitation of the first few vibrational levels. This made it possible for the second off-resonant frequency to transfer the excited molecules through the quasicontinuum region to achieve dissociation.

Attempts at high power infrared dissociation of diatomic or triatomic molecules have been unsuccessful. It appears that due to the small number of vibrational modes in these molecules no vibrational quasicontinuum is available from which dissociation can proceed.

At the present moment much theoretical and experimental work is being carried on to elucidate the mechanism of multiphoton absorption and to develop a model which explains the phenomenon in a quantitative manner. Several recent reviews on the subject have been presented[4,5,6,13,14].

It is the aim of the present work to examine an infrared laser-induced decomposition reaction in order to gain some insight into the processes described above. The molecule selected for study was ethylene. It is an easily obtained compound with a relatively simple structure and absorbs strongly in many parts of the spectral range of a carbon dioxide laser. These features make ethylene an attractive candidate for isotope separation. The thermal and photochemical reactions have been extensively studied and serve as a basis of comparison for the laser-induced decomposition.

IV. Summary of Ethylene Decomposition by Non-Laser Methods

a) Thermal Pyrolysis

The thermal pyrolysis of ethylene has been studied by several workers for temperatures of 500-600°C and pressures of 10-600 torr[15-20]. The major products found were ethane, propylene, butene, and butadiene. At higher pressures polymeric substances were formed.

The observations were explained by a free radical chain process initiated by

$$C_2H_4 + C_2H_4 \rightarrow C_2H_3 + C_2H_5 \qquad (1)$$

Ethane was formed by abstraction of ethylene by ethyl radical. Polymerization by radical addition to ethylene accompanied by decomposition resulted in the formation of the unsaturated products. The amount of polymerization was enhanced with increasing pressure and decreasing temperature.

b) Shock Tube Pyrolysis

Pyrolysis at high temperature can be achieved by means of the shock tube technique. The kinetics of ethylene decomposition at 1200-1900°C[21-25] show marked differences from the pyrolysis at lower temperature. The products are mainly acetylene and hydrogen with small amounts of butadiene. It has been suggested that the molecular dissociation process

$$C_2H_4 \rightarrow C_2H_2 + H_2$$

which was not important at lower temperatures plays a part in the reaction. Recent studies[25] show that both molecular and radical processes occur.

c) Ultraviolet Photolysis

In contrast to thermolyses, photolytic processes are initiated by energy in the form of photons specifically absorbed in one transition of the reacting species while all other modes remain unexcited. Thermal reactions proceed from systems in which energy is partitioned in a Boltzmann distribution. One might, therefore, expect basic differences in the results of photolytic and thermal decomposition reactions.

Photolysis of ethylene using ultraviolet light sources

has been well studied[26-33]. The major products were hydrogen, acetylene, ethane, and butane. Two primary processes, one molecular, the other radical were found to be about equally important:

$$C_2H_4 + h\nu \rightarrow C_2H_2 + H_2 \quad (2)$$

$$C_2H_4 + h\nu \rightarrow C_2H_3^* + H \quad (3)$$

Since butadiene was not detected in the products it was concluded that vinyl radicals produced in reaction (3) were unstable and dissociated rapidly:

$$C_2H_3^* \rightarrow C_2H_2 + H \quad (4)$$

The production of butane and ethane was explained by

$$H + C_2H_4 \rightarrow C_2H_5 \quad (5)$$

$$2C_2H_5 \rightarrow C_4H_{10} \quad (6)$$

$$\rightarrow C_2H_4 + C_2H_6 \quad (7)$$

Photolysis of equimolar mixtures of C_2H_4 and C_2D_4 yielded equal amounts of H_2 and D_2 with almost no formation of HD. This indicates that hydrogen is formed solely from the molecular reaction (2).

In a study of the flash photolysis of ethylene using a flashlamp with the spectral distribution 1500-1900Å, the major products were acetylene, hydrogen, ethane, propane, butane, and methane in decreasing order of importance. As in the other studies, an excess in the yield of acetylene over hydrogen was observed indicating that radical primary process (3) was occurring. Propane, ethane, and methane were found to be much more important

than in the low intensity photolyses discussed above. To explain these results, it was proposed that in addition to steps (2) to (7), a hydrogen atom "cracking" process occurred:

$$H + C_2H_5 \rightarrow C_2H_6^* \rightarrow 2CH_3 \qquad (8)$$

Following this, radical combination was proposed to yield propane, ethane, and methane:

$$CH_3 + C_2H_5 \rightarrow C_3H_8 \qquad (9)$$

$$CH_3 + C_2H_5 \rightarrow C_2H_4 + CH_4 \qquad (10)$$

$$2CH_3 \rightarrow C_2H_6 \qquad (11)$$

$$H + CH_3 + M \rightarrow CH_4 + M \qquad (12)$$

It appears that for the high intensity photolysis the concentration of ethyl radicals becomes great enough to compete with ethylene for hydrogen atoms and steps (8) to (12) become important.

Above 10 torr reactant pressure minor yields of propylene and butene were detected giving evidence that vinyl radicals arising from process (3) were stabilized:

$$C_2H_3^* + M \rightarrow C_2H_3 + M \qquad (13)$$

$$C_2H_3 + CH_3 \rightarrow C_3H_6 \qquad (14)$$

$$C_2H_3 + C_2H_5 \rightarrow C_4H_8 \qquad (15)$$

d) Radiolysis and Electric Discharge

In a radiolysis the reactant molecules are bombarded with high energy radiation which produces ionization. Electric discharges are induced in gases by applying a high potential difference. Ionization occurs in the gas and electrons

accelerated in the electric field collide with molecules producing further excitation and ionization. Reactions induced by radiolysis or electric discharge can proceed from excited molecules, as in photochemical reactions, or from ion-molecule reactions.

Similar conditions can be produced by infrared laser radiation of sufficiently high intensity. Electrical breakdown of the gas may occur accompanied by a flash of light from excited ions and radicals formed in the process. The reactions produced by radiolysis and electric discharge may be comparable to reactions produced by laser-induced "optical breakdown".

Radiolysis of ethylene using electron bombardment or gamma rays[34,35] have produced similar product distributions to those of the ultraviolet photolysis. The major products, acetylene, hydrogen, ethane, and butane, appear to arise from excited ethylene molecules via processes analogous to steps (2) to (7) outlined above. Methyl radicals arising from an ion-molecule reaction sequence lead to production of lesser amounts of propane and methane.

Decomposition of ethylene under electric discharge[36-40] gives hydrogen and acetylene as the major products. Other significant products whose relative importances depend on discharge conditions and pressure are ethane, propane, methane, butane, propylene, and solid polymeric deposits. From discharge spectra and esr and scavenger studies, the presence of a profusion of radicals in the discharge has been detected including C_2 and CH.

V. Infrared Laser-Induced Decomposition of Ethylene

a) Continuous Wave Laser Decompositions

Bell et al[41] using a focussed 8 watt continuous wave (CW) CO_2 laser decomposed high pressures of ethylene. At 760 torr the major products were hydrogen, acetylene, butadiene, ethane, and methane. The authors noted an increase in methane at the expense of butadiene as radiation time increased suggesting that methane was a secondary product arising from pyrolysis of butadiene. It was noted that the products were similar to those for high-temperature pyrolysis and concluded that a similar mechanism existed for the laser decomposition.

Robinson et al[42] used an unfocussed CW CO_2 laser to irradiate unspecified pressures of ethylene. With 25 watt laser power, they noted propylene as the major product with a small amount of butadiene and benzene. With 40 watts they observed propylene, methane, butadiene, and ethane as major products.

Shaub and Bauer[7] produced homogeneous heating in a reaction vessel containing 70 torr ethylene and 10 torr SF_6. SF_6 had a higher absorption coefficient at the wavelength used and transferred energy to ethylene efficiently by collision. At an estimated average temperature of 900°K using an unfocussed 9.5 watt laser beam for 30 seconds the pyrolysis products were acetylene, ethane, methane, and other unidentified hydrocarbons.

Tardieu de Maleissye et al[43] irradiated ethylene with a focussed CW CO_2 laser. Methane, acetylene, butadiene, and hydrogen were detected as products. They proposed that the rate of the laser-induced thermal pyrolysis was controlled by transport of heat to the cell walls.

b) Studies of Absorbance, Energy Transfer, and Luminescence

Letokhov and coworkers[44] observed the rapid appearance of visible fluorescence on irradiating ethylene with a focussed pulsed CO_2 laser. The fluorescence was identified as that arising from the Swan bands of the excited C_2 radical. On further study[45] it was found that C_2 radicals were formed in both the ground and excited states. It was found that the intensity threshold for appearance of luminescence in 2 torr ethylene was around 200 megawatts/cm^2.

Absorption studies were carried out using an optoacoustic detector[46]. It was found that for 1 torr of ethylene the average number of photons absorbed per molecule increased linearly with laser intensity over the range 0.5 to 100 megawatts/cm^2. A similar dependence was observed for SF_6 which also luminesces and dissociates at higher intensities. For the triatomic molecules D_2O and OCS, which can not be made to luminesce or dissociate at intensities up to 10 gigawatts/cm^2, the average number of photons absorbed per molecule reached a maximum at 10 megawatts/cm^2. This indicates that saturation of absorption had occurred for these molecules and that excitation beyond a certain level was not possible. Linear dependence of absorption on intensity was interpreted as indicating the availability of an accessible "quasicontinuum" of high density energy levels. It was concluded for the smaller molecules for which saturation of absorption was observed, that no such quasicontinuum route to higher excitation was available.

Absorption spectra of ethylene for laser radiation from 930-960 cm^{-1} at various intensities were obtained and compared to the linear absorption spectrum (spectrum at low intensity where Beer's law is applicable). From 7 to 10 megawatts/cm^2, in addition to an absorption peak centred at 949.5 cm^{-1} corresponding to Q branch absorption in the linear spectrum, two new strong absorption peaks appeared. At higher intensities the three peaks broadened and smoothened out and at 1800 megawatts/cm^2 one of the peaks at 953.5 cm^{-1} became the most prominent. The distorted symmetric top structure of the ethylene molecule gives rise to a complex superposition of rotational subbands in the vibrational energy levels of the ν_7 mode. A possible mechanism for the excitation pathways through the network of vibrational-rotational energy levels was worked out to explain the resonances observed in the high intensity absorption spectra.

Letokhov and coworkers went on to examine the correlation between luminescence intensity and laser wavelength[47,48]. Radiation from a high-pressure continuously tunable CO_2 laser of intensity 1.2 gigawatts/cm^2 was focussed into ethylene samples of less than 1 torr. The "luminescence spectrum", i.e. intensity of luminescence as a function of wavelength, was obtained. A peak in luminescence intensity was found at 953.5 cm^{-1} shifted from the Q branch linear absorption peak at 949.5 cm^{-1}. This showed a correlation between the luminescence and the absorption spectrum at high intensity discussed above. Successive additions of buffer gas enhanced luminescence intensity and broadened and

shifted the profile of the luminescence spectrum. Beyond a certain pressure of buffer gas, the intensity of luminescence began to decrease. The authors attributed this to result from the V-T/R transfer rate (rate of transfer of vibrational energy to translational and rotational degrees of freedom) becoming comparable with the laser pulse duration.

Analysis of dissociation products on irradiation of low pressures of ethylene revealed the presence of acetylene and ethane. The threshold for dissociation deduced from the appearance of acetylene in the infrared absorption spectrum was about 700 megawatts/cm^2. Luminescence was found to accompany the formation of products. It was observed that efficiency of decomposition corresponded with the luminescence spectrum.

It has been proposed that at intensities where power broadening is not large, excitation will be limited to only a comparatively small fraction of reactant molecules. Only those molecules having the proper rotational levels to be in resonance with a transition corresponding to the laser frequency will be excited. This leads to the so-called "bottleneck" effect where the excitation rate of molecules is limited by collision-induced relaxation of the rotational states of excited molecules.

The Russian workers have studied the role of rotational states in multiphoton absorption. An experiment was reported[49] on the probing of the population of rotational states at the moment when a strong CO_2 laser pulse interacted with SF_6, C_2H_4, and SiF_4 molecules. The simultaneous absorption decrease at a number of vibrational-rotational transitions was interpreted as

the result of depletion of a large number of rotational states by the laser pulse of very narrow frequency width. In a second experiment[50] absorption by 0.5 torr ethylene at 953 cm^{-1} was measured as a function of laser pulse duration, keeping the pulse energy constant. It was found that at the moderate intensity of 1 megawatt/cm^2 or greater, the average number of photons absorbed per molecule was independent of pulse length for the range 15 nanoseconds to 15 microseconds. This covers a collision-free to collisional time span. Since absorption was the same whether collisions were absent or present, it was concluded that a large number of rotational states can be excited. Thus it appears from these experiments that rotational relaxation is not required for multiphoton absorption.

c) Pulsed Infrared Laser Dissociation

Bastiaens, de Keuster, and de Hemptinne[51] irradiated ethylene using a TEA CO_2 laser delivering pulses of 1 to 3 joules and 150 nanosecond duration. The irradiations were performed in a 150 cm^3 reaction vessel connected to a digital pressure gauge. For ethylene pressures above 5 torr, using a focussed beam, optical breakdown accompanied by a pressure rise occurred with every pulse. Analysis of the products by gas chromatography revealed the presence of only hydrogen and acetylene. After one to two hundred pulses the total gas pressure reached a constant value. The pressure change indicated that about 85% of the ethylene was converted to acetylene. Irradiation of acetylene-hydrogen mixtures resulted in a pressure decrease which reached a maximum at a pressure corresponding to formation of 15%

ethylene. The authors concluded that the equilibrium

$$C_2H_4 \rightleftarrows C_2H_2 + H_2$$

was achieved in the reaction mixture.

A spectral investigation of the luminescence accompanying breakdown showed that the main emission came from excited hydrogen molecules. Luminescence with a shorter lifetime from an unidentified organic species was also noted.

When unfocussed radiation was used, no breakdown or reaction products were detected. The authors were able to induce the reaction of ethylene with HCl giving ethyl chloride using an unfocussed beam at 939 cm^{-1}. C_2D_4-DCl mixtures gave no reaction since C_2D_4 did not absorb the laser frequency. However, irradiation of C_2H_4-C_2D_4 mixtures with HCl or DCl gave reaction in which deuterated ethylene reacted preferentially.

When the low ethylene pressures of 0.1 to 0.3 torr were irradiated with a focussed beam at 939 cm^{-1}, slow production of hydrogen was noted which increased linearly with the number of laser pulses. No luminescence was observed at these pressures. The hydrocarbon products of the reaction could not be identified, but the authors were unable to detect acetylene. Irradiation of a 0.25 torr mixture of C_2H_4-C_2D_4 resulted in preferential reaction of C_2H_4.

In another study Peterson, Manning, and Braun[52] photolyzed 1% ethylene in helium at total pressures of 50-200 torr using focussed CO_2 laser radiation. The only products detected by gas chromatography were hydrogen and acetylene. No

luminescence was observed. As the pressure of inert gas was increased the efficiency of the decomposition was found to be enhanced. The authors concluded that the reaction occurred exclusively via molecular elimination of hydrogen from ethylene. The lack of products other than hydrogen and acetylene was cited as evidence that no hydrogen atom elimination processes took place.

d) Summary and Object of the Present Work

The earlier CW laser decompositions which involved continuous, relatively low intensity radiation clearly proceeded by a mechanism of thermal pyrolysis. Of more interest in the field of laser-induced chemistry is the use of pulsed radiation where it is possible for selectivity of the excitation to be maintained and reflected in the chemistry.

Study of the infrared-induced dissociation of ethylene using pulsed lasers has been limited. Most of the emphasis has gone into the study of absorption processes with only a cursory examination of the reaction products. In order to understand the chemistry of the process, a detailed chemical analysis of the reaction products is required. This has been the object of the present work. Product distributions under conditions of varying reactant pressure and incident radiation intensity have been determined using mass spectral indentification and quantitative gas chromatographic analysis.

In particular the nature of the primary processes for the infrared-induced dissociation has not been resolved. Thermal pyrolyses and ultraviolet photolyses have involved both molecular

and radical primary processes. From the limited studies of pulsed infrared laser dissociation of ethylene to date, the importance of molecular or radical processes is not clear. This is necessary for an assessment of the potential for separation of isotopes.

A useful tool in mechanistic studies is the employment of isotopically substituted reactants. Mixtures of C_2H_4 and C_2D_4 have been used in the present study to elucidate the reaction mechanism and to investigate isotope selectivity.

Chapter Two: Experimental

I. Irradiation System

The arrangement for a typical irradiation experiment is illustrated in Figure 1. Irradiations were carried out using a Lumonics Model 103 TEA carbon dioxide laser. A continuous gas flow consisting of a mixture of helium, carbon dioxide, and nitrogen in the ratio of 92:5:3 was passed through the laser cavity at atmospheric pressure. The gases were excited by a high voltage supplied across electrodes arranged transversely to the laser cavity. The pulse width of the output beam at half maximum intensity was about 250 nanoseconds. The maximum energy of the laser pulse was about 5 joules and the pulse rate was 35 to 45 pulses per minute (0.6 to 0.75 Hz). The laser was line-tuned by means of a rotatable gold-coated diffraction grating situated at one end of the laser cavity. A precise vernier measured the angle of rotation of the grating. Vernier settings were calibrated using a Lumonics CO_2 laser spectrum analyzer so that the desired wavelength of laser radiation could be selected by setting the vernier at the appropriate reading. Beam energy was measured by a calibrated pyroelectric detector constructed by Lumonics Research Limited. The active component of the detector was a ceramic crystal which absorbed incident light. The resulting temperature increase of the crystal was converted to an electric signal displayed on an oscilloscope (Tektronix type 545).

To achieve uniformity of the beam shape a beam constrictor was placed in the beam path. This consisted of a

Figure 1

Arrangement for a typical irradiation experiment

La - CO_2 TEA laser

M - gold-coated mirrors

BC - beam constrictor

BS - beam splitter

OD - optoacoustic detector

L - germanium lens

RV - reaction vessel

B - carbon backstop

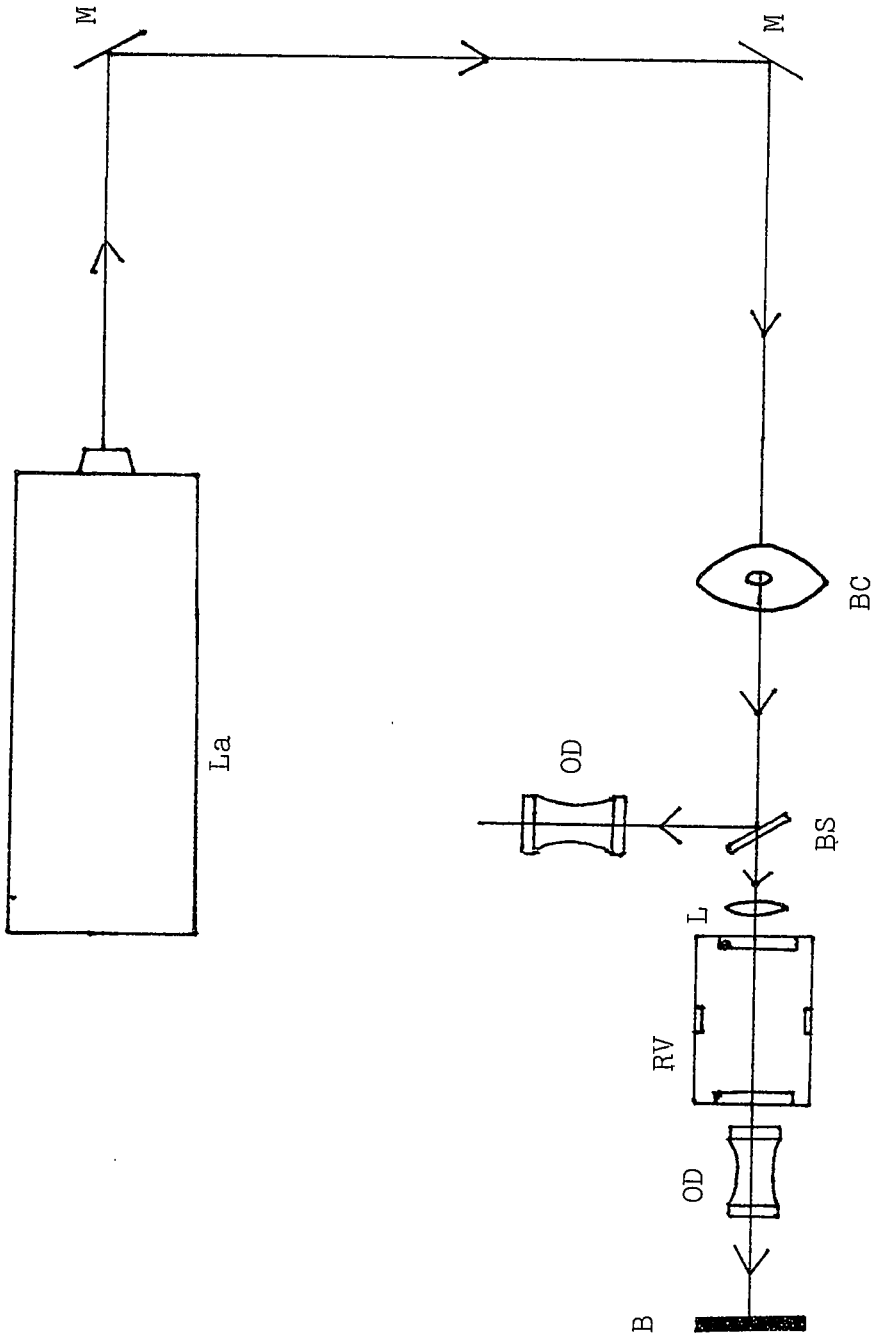
M
M
La
BC
OD
BS
L
RV
OD
B

mounted metal disc with a half-inch diameter hole drilled through the center. By means of a pyroelectric detector, it was found that 25% of the beam energy was transmitted through the constrictor when the gold-coated mirrors were adjusted so that the central portion of the laser beam passed through the aperture. The laser beam was focussed by means of an anti-reflective coated germanium lens of 4.0 cm focal length placed in front of the reaction vessel.

To monitor the laser output during an irradiation an optoacoustic detector illustrated in Figure 2 was used. The detector consisted of a pyrex cell with sodium chloride windows filled with ethylene. A microphone with connections to an oscilloscope was set within the cell so that pressure changes produced by absorption of the laser radiation by ethylene in the cell would be detected. Optimal sensitivity of the detector was achieved with 125 torr of ethylene.

The detector gave a linear response to light intensity. This was demonstrated by the use of wire gauzes of varying mesh sizes. The transmittances of the gauzes at the visible wavelength 5711 Å were determined using a Cary Model 14 Spectrophotometer. These transmittances were found to be proportional to the transmittances measured by the change in the microphone signal when the gauzes were placed in the path of the laser beam.

A beam splitter consisting of a sodium chloride plate was placed in front of the reaction vessel. It transmitted approximately 95% of the laser beam to the reaction vessel and

Figure 2

Optoacoustic Detector

I - inlet for gas introduction

W - sodium chloride window

M - microphone

T - tungsten leads to oscilloscope

Figure 3

Reaction Vessel

C - Kovar to glass connection to vacuum line

R - threaded brass ring

T - teflon ring

O - O-ring seal

W - sodium chloride window

Q - quartz window

Figure 2

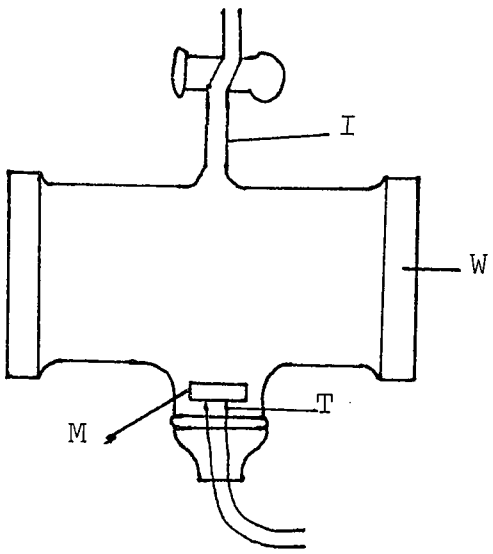

Figure 3

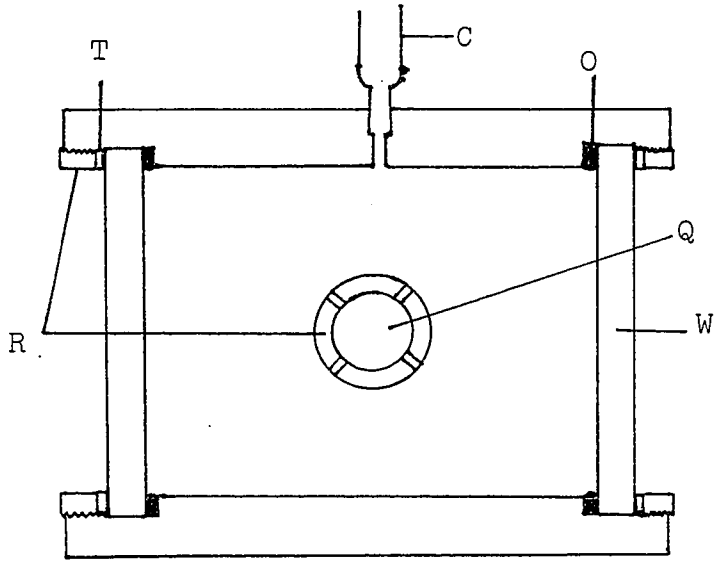

deflected the remainder to the optoacoustic detector. To measure the absorption of the laser radiation by ethylene in the reaction vessel, a second optoacoustic detector was placed behind the cell.

Figure 3 is a diagram of the reaction vessel used for most of the experiments. It was constructed of brass with a length of 10 cm and inner diameter 4.5 cm. The volume of the cell plus a small glass connecting tube was 112 ml. Windows were recessed into the cell and made vacuum-tight contact against rubber O-rings resting in circular grooves. The front and rear windows were sodium chloride, 5 cm in diameter and 6 mm thick. Quartz side windows were installed for observation of visible luminescence produced during irradiations.

For some early experiments a 5 cm long brass cell with germanium windows in front and rear was used in combination with an antireflective coated germanium lens of focal length 3.0 cm.

Sodium chloride components were covered with plastic bags containing silica gel desiccant when not in use. Cell windows were cleaned and polished to remove film, carbon deposits, or damage spots which were sometimes created during irradiations.

II. Vacuum Apparatus

The reaction vessel was connected to a grease-free vacuum system illustrated in Figure 4. The cell and vacuum line were evacuated to less than 10^{-4} torr before an experiment using a rotary oil pump (Welch Duo-Seal model 1400) in series with a mercury diffusion pump. Pressure measurements in the vessel were

Figure 4

Vacuum and Analysis System

1. rotary oil pump
2. mercury diffusion pump
3. liquid nitrogen trap
4. McLeod gauge
5. gas inlet
6. mercury manometer
7. gas storage bulbs
8. main vacuum line manifold
9. Wallace & Tiernan pressure gauge
10. brass manifold
11. reaction vessel
12. 3/16" O.D. copper connecting tube
13. 1/4" O.D. copper sample loop
14. 4-port Lorenco valve
15. helium supply
16. Hewlett-Packard gas chromatograph
17. glass tube trap for condensible products
18. solid nitrogen trap
19. Toepler pump/gas buret
20. column for hydrogen analysis
21. Gow-Mac gas chromatograph
22. tube crusher
23. Perkin Elmer gas chromatograph
24. Hitachi mass spectrometer

⊠ metal Hoke valve

X glass stopcock

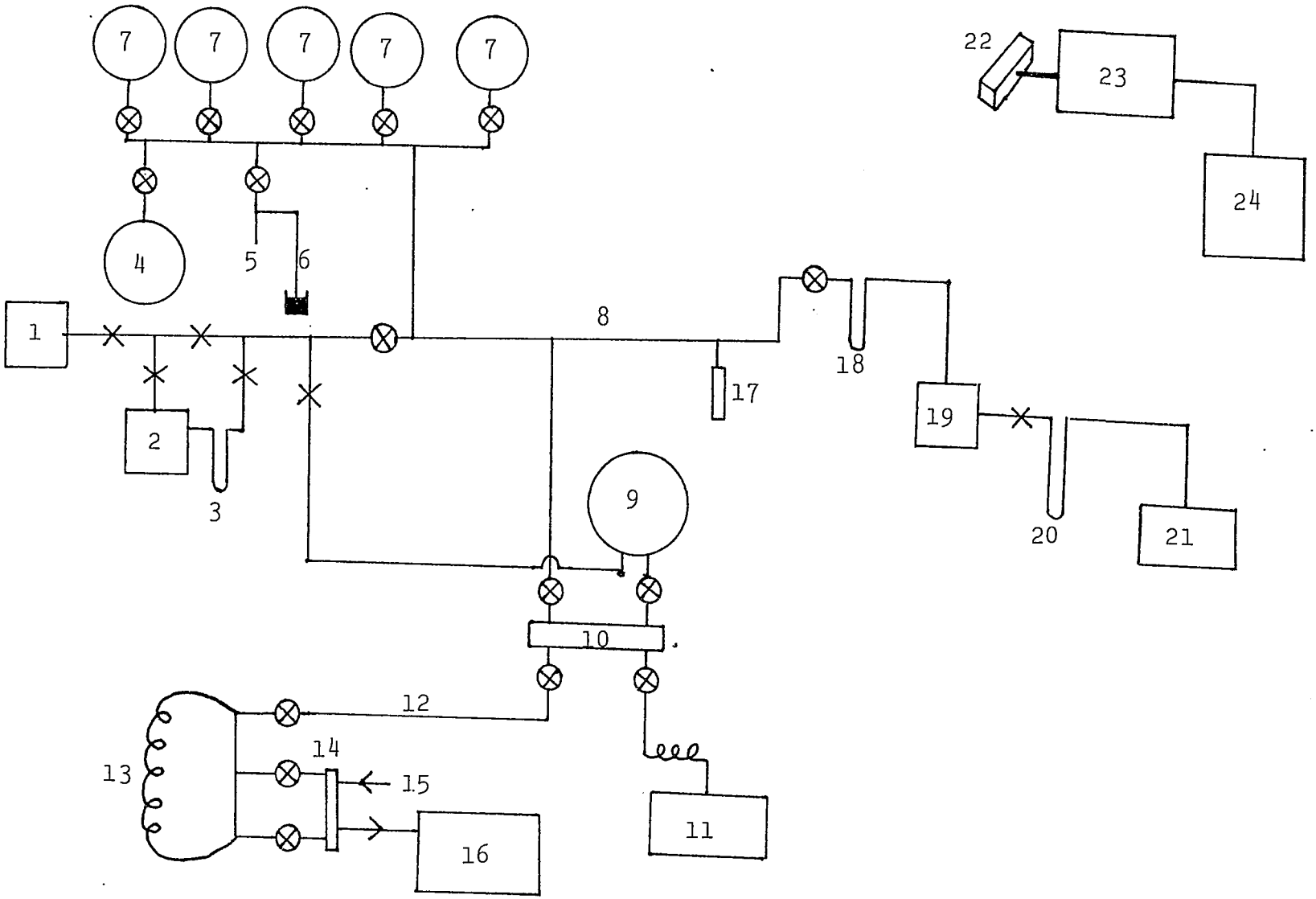
7
7
7
7
7
4
5
6
1
8
22
23
24
18
17
19
2
3
9
20
21
10
12
13
14
15
16
11

made from 0.5 to 220 torr using a Wallace & Tiernan pressure gauge (model FA145) and from 0 to 0.4 torr using a McLeod gauge.

III. Analytical System

A 1/4" O.D. copper sample loop of volume 35 ml was connected to the cell manifold via a 3/16" O.D. copper connecting tube (Figure 4). For a series of analyses, the contents of the cell were expanded directly into the sample loop. Connections were made via a 4-port Lorenco valve (Figure 5) into a Hewlett-Packard F&M Model 700 gas chromatograph with a flame ionization detector. Calibrations were made by introducing measured pressures into the reaction vessel which were then expanded into the sample loop in the same way as for the reaction products.

In a second series of experiments, the hydrogen products were separated by passing the contents of the reaction vessel through a solid nitrogen trap. Condensible hydrocarbon products were sealed in glass tubes for analysis on a Perkin Elmer model 990 gas chromatograph with a flame ionization detector. This chromatograph was interfaced with a Hitachi RMU-6D mass spectrometer for identification of the products.

Hydrogen was collected in a gas buret by means of a Toepler pump. The isotopic hydrogen species were then separated on a column leading to a copper oxide oven maintained at 300°C where the products were converted to water. Analysis was then carried out using a gas chromatograph with a detector of Gow-Mac W-2 thermal conductivity filaments.

Figure 5

Sample Introduction System

L - sample loop

X - metal Hoke valves

connections:

He - helium supply

GC - gas chromatograph

V - vacuum line and reaction vessel

(a) Valve in

Evacuation of sample loop via vacuum line or introduction of sample from reaction vessel

(b) Valve out

Transfer of sample to gas chromatograph

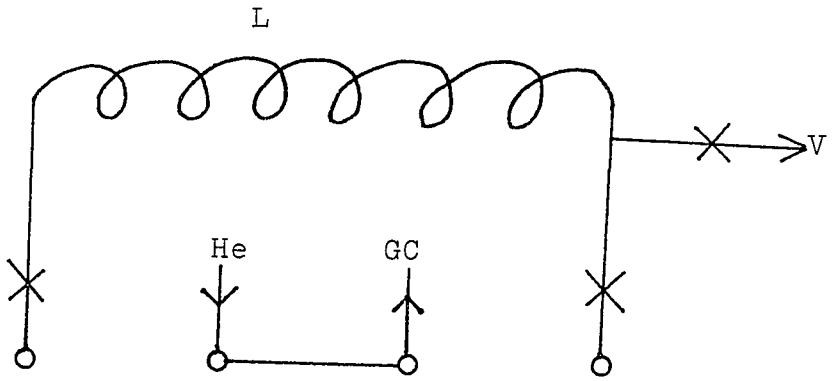

(a)

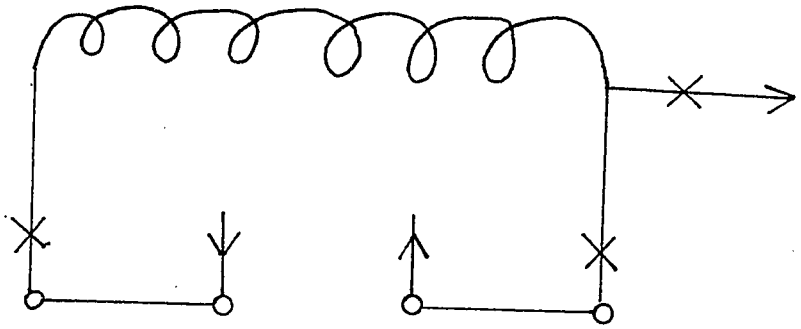

(b)

IV. Columns used in Gas Chromatography

For determination of methane, ethane, ethylene, acetylene, butane, and propylene, a 6 meter 1/4 inch O.D. copper column of phenylisocyanate on porasil was used at room temperature. Unsaturated C-3 and C-4 hydrocarbons were measured on 1/4 inch O.D. copper columns of n-octane on porasil. Either a 3 meter column at room temperature or a 6 meter column at 60°C was used. In some analyses these columns were programmed to 100°C and no significant amounts of products having carbon number greater than 4 were detected.

The isotopic species of hydrogen were analyzed using a glass column of activated alumina treated with $MnCl_2$ and kept at liquid nitrogen temperature.

V. Calibrations

With the use of the F&M gas chromatograph, calibration curves of peak height as a function of amount of gas were obtained for methane, ethane, propane, and acetylene. Product amounts were determined from the peak heights corresponding to these compounds on the gas chromatogram of the products using the calibration curves. For the other products, which had longer retention times, peak areas were measured and divided by carbon number. Peak area ÷ carbon number was also obtained for acetylene and propane. Using the known amounts of these compounds from the calibration, a conversion factor for peak area ÷ carbon number to micromoles of product was obtained from which the amounts of the other compounds were calculated. The limit of

detectability was about 2 nanomoles for the lighter hydrocarbons and was somewhat larger for the heavier products. Calibrations were not made using the Perkin Elmer gas chromatograph. For experiments involving the use of this instrument, peak area ÷ carbon number values were used as a basis of comparison for the relative amounts of products.

Due to large variations in retention time and sensitivity for hydrogen products on the gas chromatographic system from day to day, calibrations were made immediately before or after the analysis of products from each irradiation experiment. Calibration was achieved by introducing a measured amount of pure H_2 or of an H_2-HD-D_2 mixture of known composition of roughly the same proportions as those for the hydrogen products of the irradiation. Product yields were obtained from comparison of peak heights of the products to those of the calibration gases. The limit of detectability for the hydrogen products was about 40 nanomoles.

VI. Materials

Hydrocarbon gases used in calibrations were Matheson C.P. grade with a stated minimum purity of 99.0%. Ethylene used in the laser experiments was Matheson Research grade with a stated minimum purity of 99.98%. Further purification was achieved by repeated degassing at liquid nitrogen temperature. Traces of methane and ethane impurities less than 20 ppm were detected. The ethylene-d_4 used was from Merck Sharp & Dohme with a stated isotopic purity of 99%. High-purity gases were

used in the calibrations of the hydrogen species: H_2 from Matheson assayed as 99.9995% pure, D_2 from Bio-Rad Laboratories with a minimum mole percentage of 99.65%, and HD from Merck Sharp & Dohme with a stated minimum isotopic purity of 98%. High-purity Matheson helium and nitrogen were used in the studies with inert gas additives.

Chapter Three: Results and Discussion

I. Absorption Spectra

The absorption spectra of C_2H_4 and C_2D_4 were measured for the frequency range of the CO_2 laser emission (900-1100 cm^{-1}). A Perkin Elmer Model 621 Grating Infrared Spectrometer was used. Parts of the spectra are shown in Figures 6 and 7.

The absorption for C_2H_4 corresponds to the ν_7 bending vibration (Figure 6). The laser lines used in irradiation experiments were the P(14) (949.5 cm^{-1}) and P(26) (938.7 cm^{-1}) lines of the 00°1-10°0 transition of CO_2. These two frequencies lie in a strongly absorbing Q branch of the absorption band of C_2H_4. Product yields using the two lines were not greatly different. Absorption by C_2D_4 was not detectable for the frequency range 930 to 1020 cm^{-1}.

The absorption peak of C_2D_4 centered at 1080 cm^{-1} (Figure 7) is the Q branch of the ν_{12} CD_2 deformation vibration. The CO_2 laser line R(22) of the 00°1-02°0 transition lies at the center of the absorption peak.

II. Absorbance as a Function of Pressure

The absorbance of the P(26) laser line by ethylene was measured in a pyrex vessel with sodium chloride windows. The voltage signal from a pyroelectric detector placed behind the cell was measured as increments of pressure were added. Percent transmittance was obtained from the ratio of the detector signal with added gas (I), to that with the cell evacuated (I_o). A plot of absorbance ($\log \frac{I_o}{I}$) as a function of pressure is shown

Figure 6

Absorption Spectrum of C_2H_4

Positions of laser lines used in experiment are indicated by arrows.

Cell length: 9 cm

Pressure: 58 torr

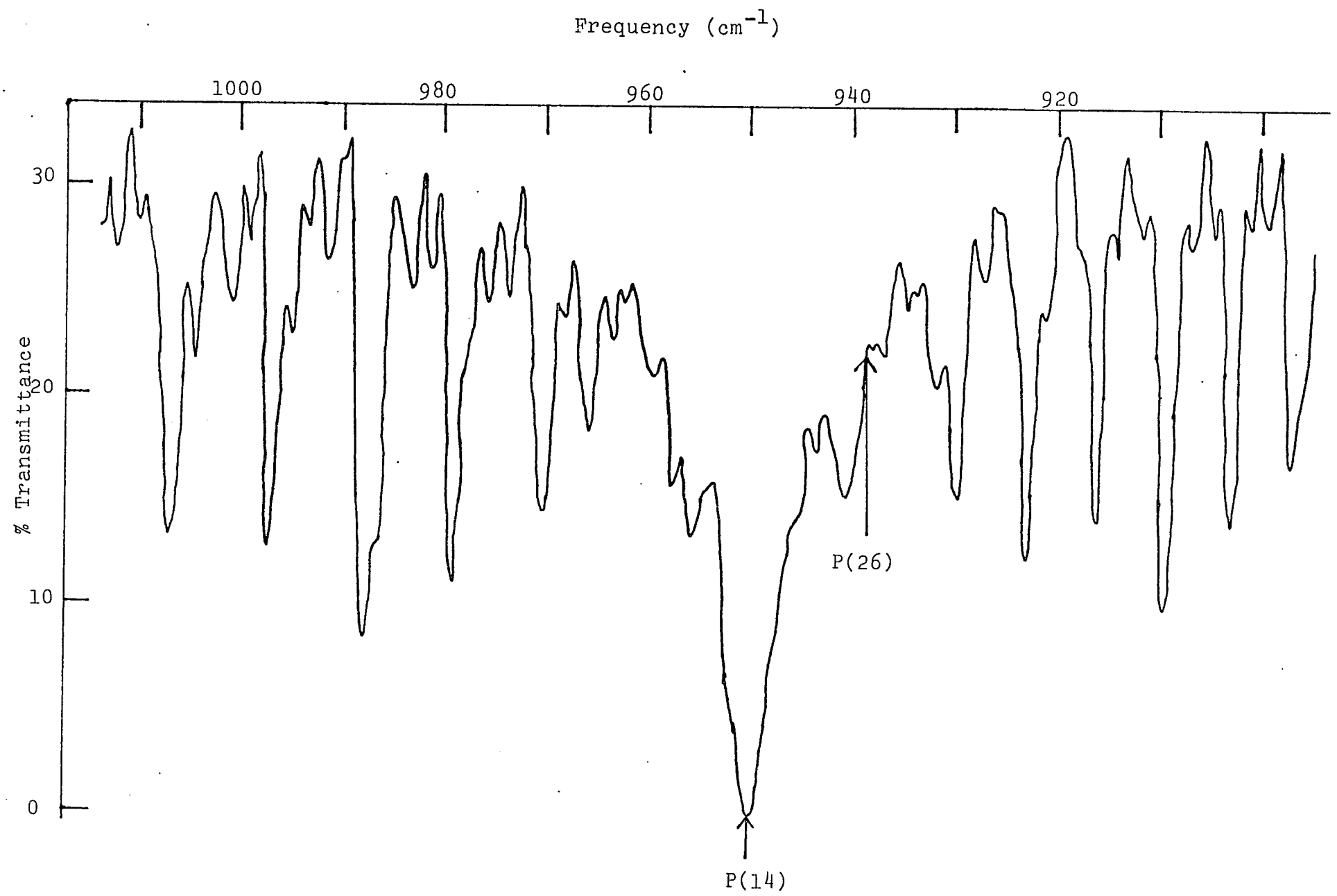
Frequency (cm-1)
1000
980
960
940
920
30
20
10
0
% Transmittance
P(26)
P(14)

Figure 7

Absorption Spectrum of C_2D_4

Position of laser line used indicated by arrow

Cell length: 9 cm

Pressure: 58 torr

Solid line: spectrum of C_2D_4

Dashed line: spectrum of C_2H_4

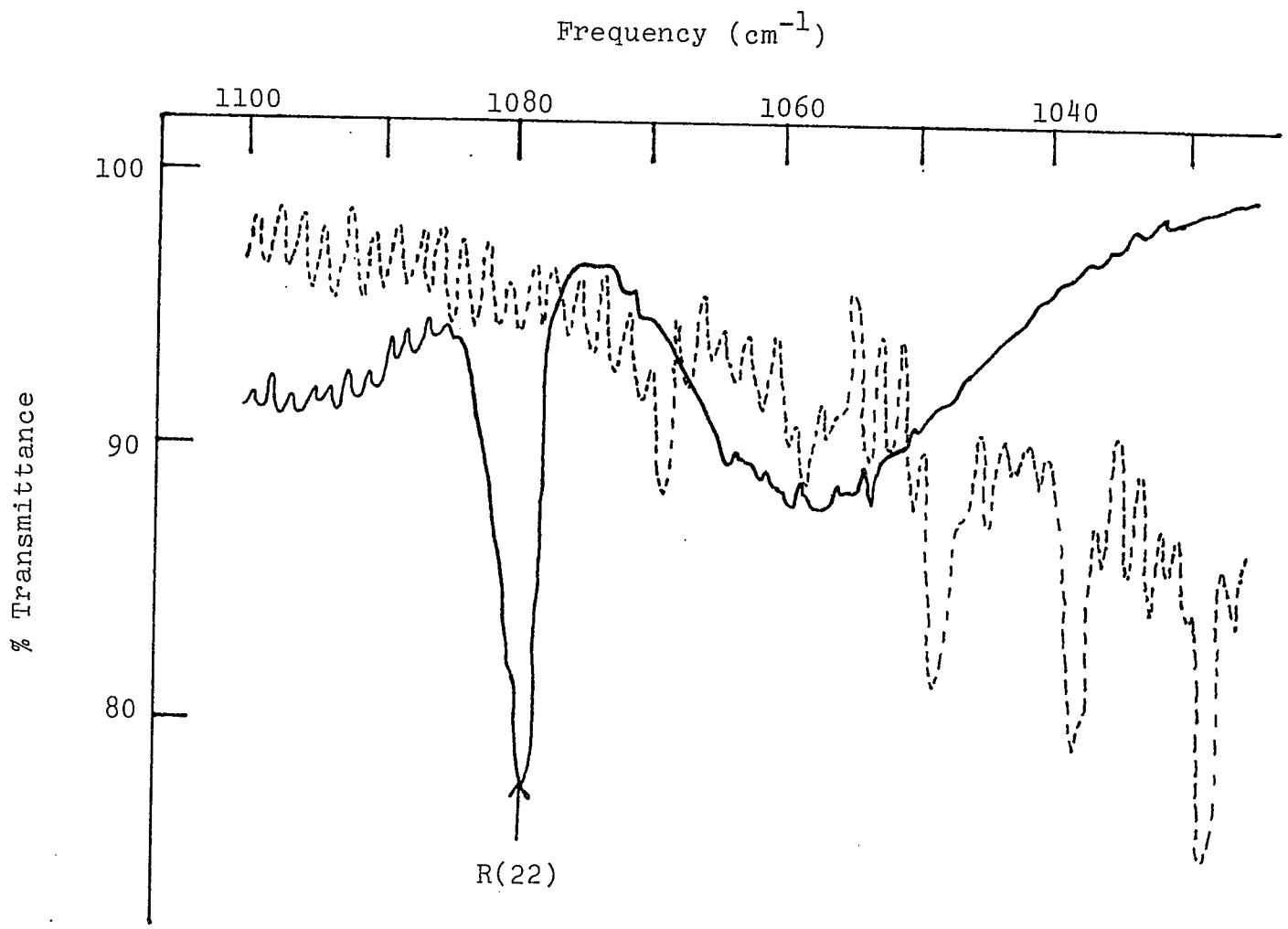
Frequency (cm^{-1})
1100
1080
1060
1040
100
90
80
% Transmittance
R(22)

in Figure 8. If the small intercept slightly to the right of the origin is disregarded, the absorbance follows a Beer's law relation from 0 to 240 torr with an extinction coefficient of 1.1×10^{-3} $torr^{-1}cm^{-1}$. Strictly speaking, since the intensity of the beam changes rapidly with time, this is an "average absorption coefficient" over the whole range of intensities found in the time profile of the pulse.

With a focussed beam, below the breakdown threshold pressure, absorbance was not large enough to measure reliably because of the sensitivity limits of the detector. With the onset of breakdown, a marked increase in absorption was noted indicating interaction of the plasma with the laser radiation. The volume in which reaction takes place is probably much smaller than the volume of gas irradiated by the beam in the cell. Therefore this type of measurement is not a very sensitive indicator of absorption behavior in the volume of reaction in the focussed beam.

III. Characteristics of the Focussed Beam

The photon flux sufficiently high for infrared laser-induced decomposition of many molecules is only present in a small region near the focal point of a focussed beam. The intensity in this "reaction volume" depends upon the cross-sectional area at the focus. The beam waist (radius of the beam at the focal point) depends on diffraction of the beam by the lens, spherical aberration of the lens, and divergence of the beam output from the laser. These are determined by such

Figure 8

Absorbance as a Function of Pressure

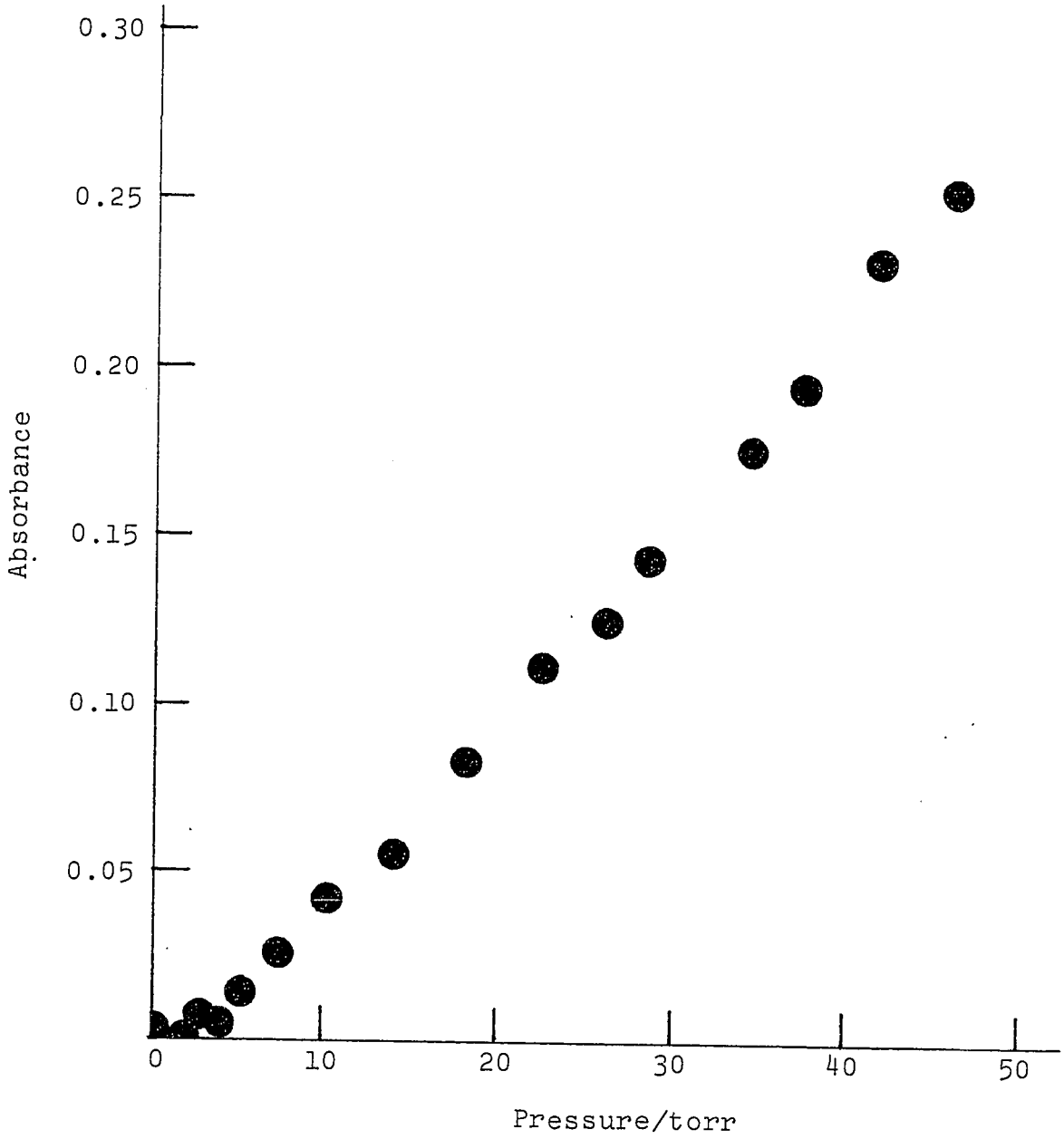
0.30
0.25
0.20
0.15
0.10
0.05
Absorbance
0
10
20
30
40
50
Pressure/torr

factors as the wavelength of the laser radiation, width of the beam as it strikes the lens, and focal length and refractive index of the lens.[53]

Relevant data for the beam and lens conditions used in this work are summarized in Table 1. A representation of the focussed beam is shown in Figure 9. The size of the beam waist is limited by the divergence of the laser beam. For a divergence-limited gaussian beam, the beam waist is approximately equal to the product of the beam divergence angle in radians and the focal length of the lens.[54] The Lumonics CO_2 TEA laser had a specified beam divergence of 1 milliradian. Thus the 4.0 cm focal length germanium lens gives a beam waist of 4×10^{-3} cm and a cross-sectional area of $\pi w^2 = 5 \times 10^{-5} cm^2$. For the laser lines used about 1.2 joules were transmitted through the beam constrictor for the laser pulse of width 250 nanoseconds. The fluence (integrated energy per unit area) and intensity (fluence per unit time) over the cross-section of the beam focus are thus calculated to be 2.4×10^4 joules/cm^2 and 1×10^{11} watts/cm^2 respectively. Energy losses due to absorption and reflection by the lens and cell window are neglected since these are small compared to the uncertainty of the calculations.

The gaussian intensity distribution applies only to the TEM_{00} mode of the laser radiation.[53] A significant contribution from higher transverse modes is present for lasers with multimode output. For the Lumonics Model 103 laser used, this may be greater than 50% of the total energy of the beam. With the use of the beam constrictor, the transmitted beam

Table 1

Focussed Beam Characteristics

energy/pulse (J)	pulse width (nsec)	beam divergence (rad)	focal length (cm)
1.2	250	1×10^{-3}	4.0

beam waist (cm)	beam X-section area at focus (cm^2)	fluence (J/cm^2)	intensity (W/cm^2)
4×10^{-3}	5×10^{-5}	2.4×10^{4}	1×10^{11}

Figure 9

Representation of the Focussed Beam

w - beam waist

b - length of focal waist

f - focal length of lens

The dimensions of the focal region have been exaggerated.

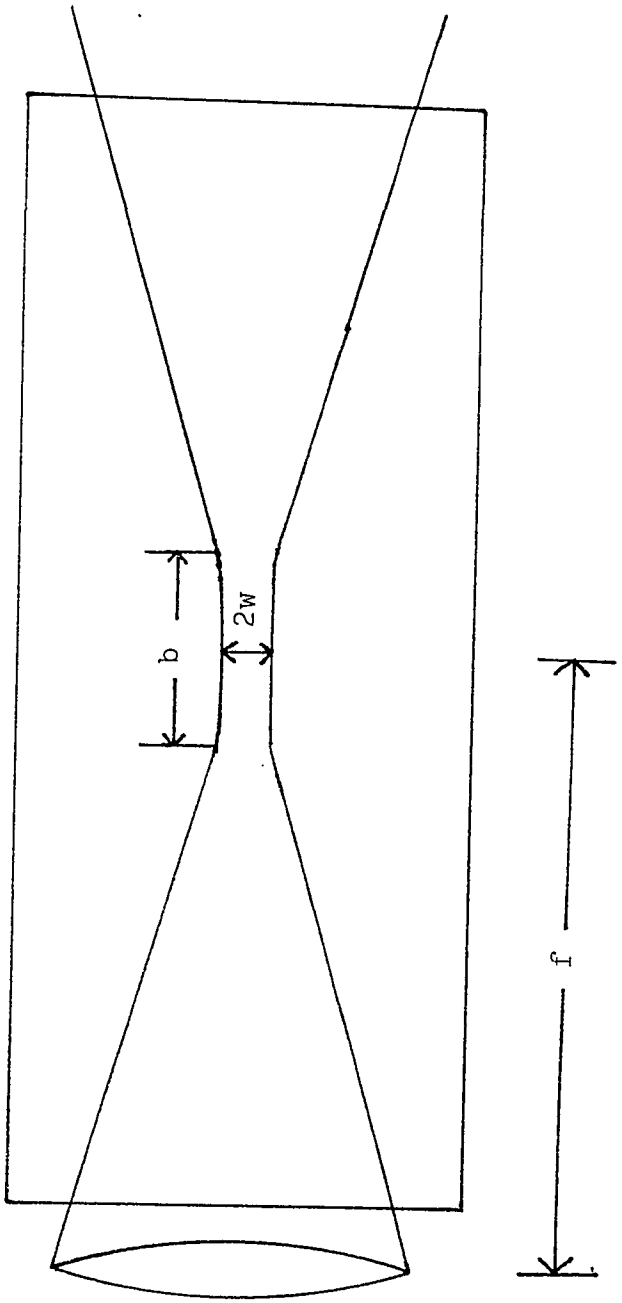
b
2w
f

consisted mainly of the fundamental transverse mode which has a spatial distribution largely in the center of the beam. Nevertheless, the gaussian energy distribution is only an approximation and the values given above are rough calculations. An accurate determination of the dimensions of the focal region requires well-defined beam conditions. Uncertainties in the geometry of the focal region of the beam often complicate interpretation of studies involving focussed laser light.

IV. Irradiation Experiments with an Unfocussed Beam

Pressures of 15, 30, 50, 80, 200, 220, and 580 torr of ethylene were irradiated with 5100 pulses of the unfocussed P(26) line. No products were detectable. Irradiation of a mixture of 50 torr ethylene and 370 torr nitrogen under the same conditions also produced no measurable products. Therefore the fluence of 0.15 joules/cm^2 and intensity of 6×10^5 watts/cm^2 are insufficient to induce decomposition of ethylene.

Table 2 shows the maximum temperature attained in the cylindrical volume of irradiation assuming complete thermalization of the absorbed energy. The calculations were made using the absorbance measurements of section II and heat capacity data from the literature.[55] Since no reaction was detected, significant loss of heat by conduction and diffusion from the irradiation zone must have occurred at the lower pressures.

V. Breakdown Threshold

With irradiation by a focussed laser beam, optical breakdown of ethylene was observed above a certain pressure.

Table 2

Predicted Temperature in Irradiation Volume Assuming Complete Thermalization of Absorbed Energy

pulse energy: 1.13 j/pulse P(26) (corrected for loss at cell window)

volume of irradiation: 7.60 cm^3

Pressure (torr)	Fraction of Energy Absorbed	Maximum Temperature (°C)
15	0.20	1020
30	0.37	860
50	0.53	790
80	0.70	690
200	0.95	565
220	0.97	540
580	1.00	335

This was indicated by a distinct flash of visible luminescence observed from the quartz side windows of the reaction vessel. The pressure threshold depended on intensity of laser radiation which was a function of the focal length of the lens.

A study was done to investigate the effect of adding inert gas on the breakdown threshold for ethylene. The percentage of pulses for which luminescence was observed is shown as a function of ethylene pressure in Figure 10. The P(26) laser line was focussed with a germanium lens of focal length 4.0 cm into the 100 ml reaction vessel. Successive increases in the mole fraction of inert gas resulted in a lowering of the pressure at which breakdown was induced in ethylene.

It is apparent that collisional processes assist the achievement of breakdown. The added pressure of the inert gas may inhibit diffusion of heat from the irradiation zone. Breakdown of the gas could occur as a result of the increased amount of time before cooling occurs. It is also possible that enhancement of absorption of laser radiation may be induced by collisions between inert gas and ethylene molecules. This may come as a result of collision broadening of absorption or collisional relaxation of excited ethylene molecules so that the anharmonicity barrier for further absorption is removed. These effects will be discussed in more detail in section VI(d).

VI. Reaction Products

(a) Product Distributions

Studies of laser-induced decomposition were made using ethylene pressures above and below the breakdown threshold using

Figure 10

Breakdown Threshold Study

Percentage of laser pulses for which luminescence was observed as a function of ethylene pressure in the reaction vessel.

● 1.3% ethylene in N_2

△ 1.3% ethylene in He

■ 11.5% ethylene in N_2

○ 80% ethylene in N_2

▲ pure ethylene

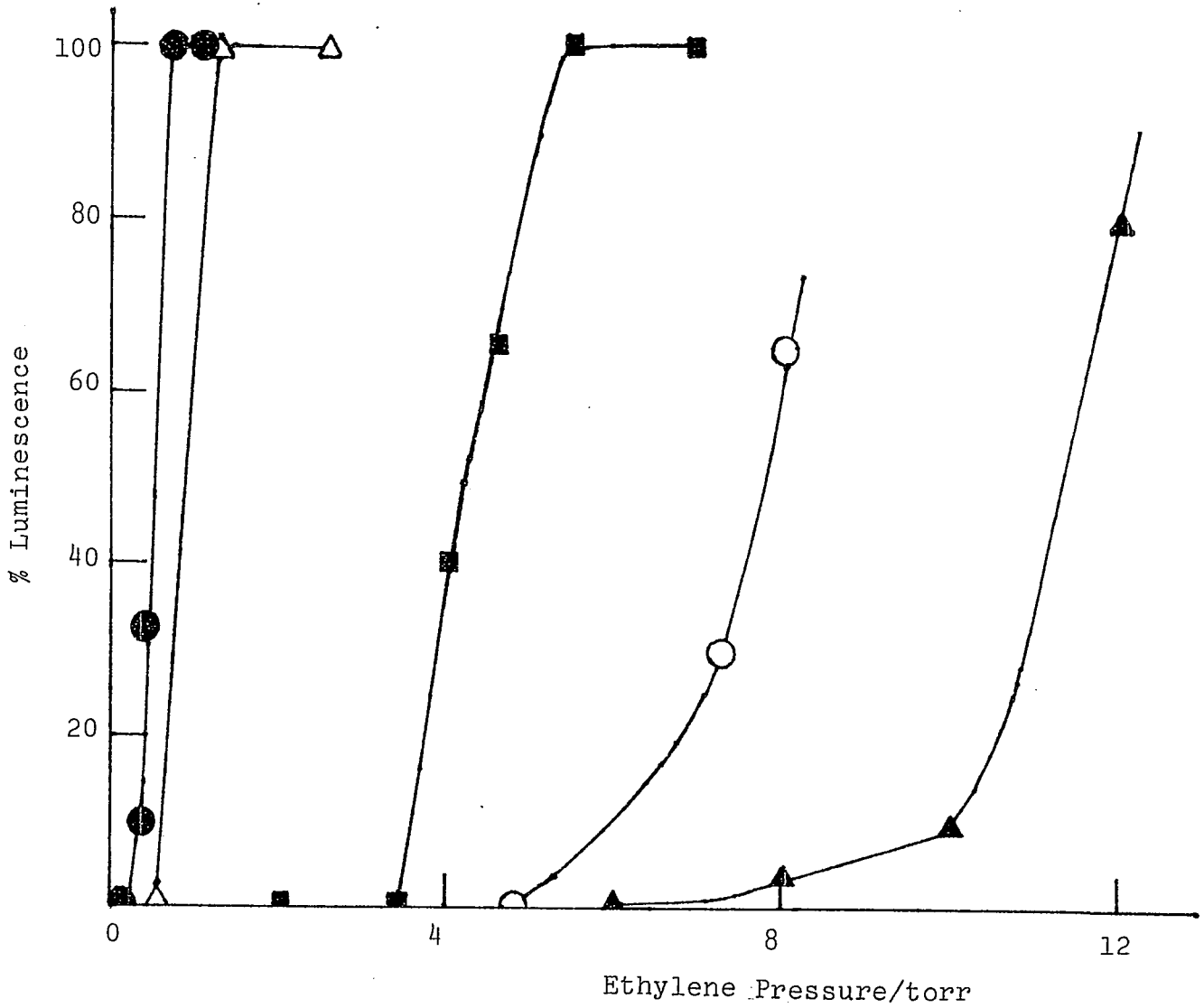
100
80
60
40
20
% Luminescence
0
4
8
12
Ethylene Pressure/torr

either the P(26) or P(14) laser line. The major products for all experiments were acetylene and hydrogen. The relative hydrocarbon yields as a function of pressure are shown in Figure 11. Under nonbreakdown conditions significant amounts of ethane, propane, propylene, and butane were produced. As the pressure of reactant was lowered, saturated hydrocarbons formed a larger proportion of the products.

Above the breakdown threshold, in addition to the products listed above, the unsaturated hydrocarbons diacetylene, butadiene, vinylacetylene, methylacetylene, butene, and ethylacetylene were formed. Relative product yields did not show significant variation for the pressure range studied.

Table 3 and Figure 12 show product distributions for a series of typical experiments using the P(26) laser line. Similar product distributions were found using the P(14) line except that for nonbreakdown conditions the ethane yield was slightly larger than the propane yield and the percentage of saturated hydrocarbons was somewhat greater (Figure 11).

(b) Yield as a Function of Irradiation Time

Figure 13 shows product yields as a function of number of laser pulses for a series of experiments done under non-breakdown conditions. The plots for product formation are linear passing through the origin indicating that all of the products are primary.

Figures 14 and 15 show product yields as a function of number of laser pulses for a series of experiments done under

Figure 11

Relative Product Yields as a Function of Ethylene Pressure

laser lines used: nonbreakdown region P(14) 949.5 cm^{-1}

breakdown region P(26) 938.7 cm^{-1}

● acetylene

△ ethane

□ propane

○ propylene + butane

■ unsaturated C-4 hydrocarbons

▲ saturated hydrocarbons

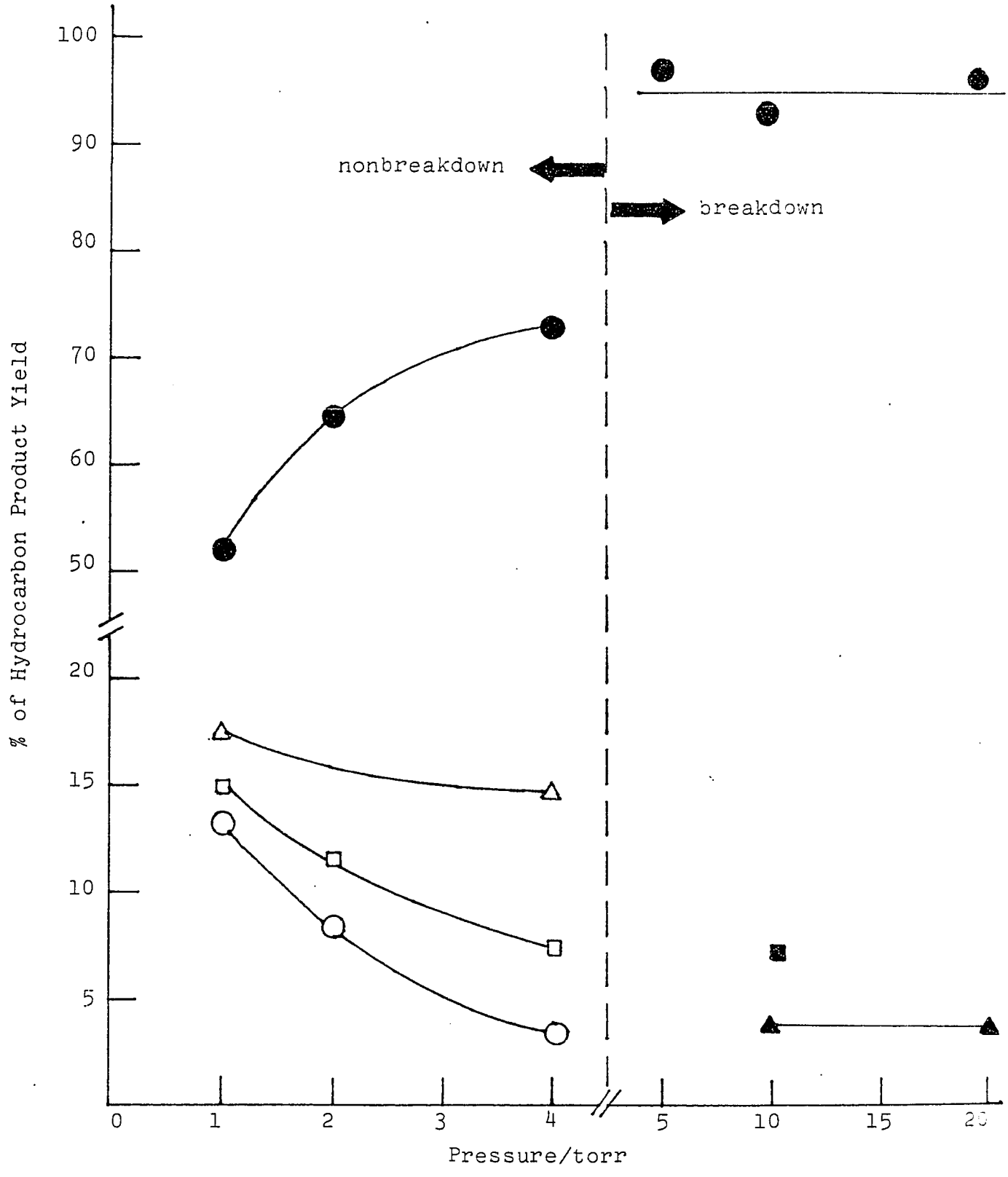
100
90
80
70
60
50
20
15
10
5
% of Hydrocarbon Product Yield
nonbreakdown
breakdown
0
1
2
3
4
5
10
15
20
Pressure/torr

Table 3

Hydrocarbon Products - Percentage of Product Yield

Nonbreakdown (4 torr)		Breakdown (10 torr)			
Product	% Yield	Product	% Yield	Product	% Yield
acetylene	79.5	acetylene	92.9	unsaturated C-3 &	7.07
total saturated hydrocarbons	20.3	total saturated hydrocarbons	4.19	C-4 hydrocarbons	
methane	1.25	methane	1.90	propylene	0.23
ethane	6.35	ethane	1.08	methylacetylene	0.06
propane	8.13	propane	0.88	diacetylene	5.87
butane	4.33	butane	0.33	butadiene	0.54
propylene	0.29			vinylacetylene	0.31
				butenes *	0.05
				ethylacetylene	0.04

* 1-butene, cis-2-butene, trans-2-butene, and isobutene were not resolved

Figure 12. Typical Product Distributions

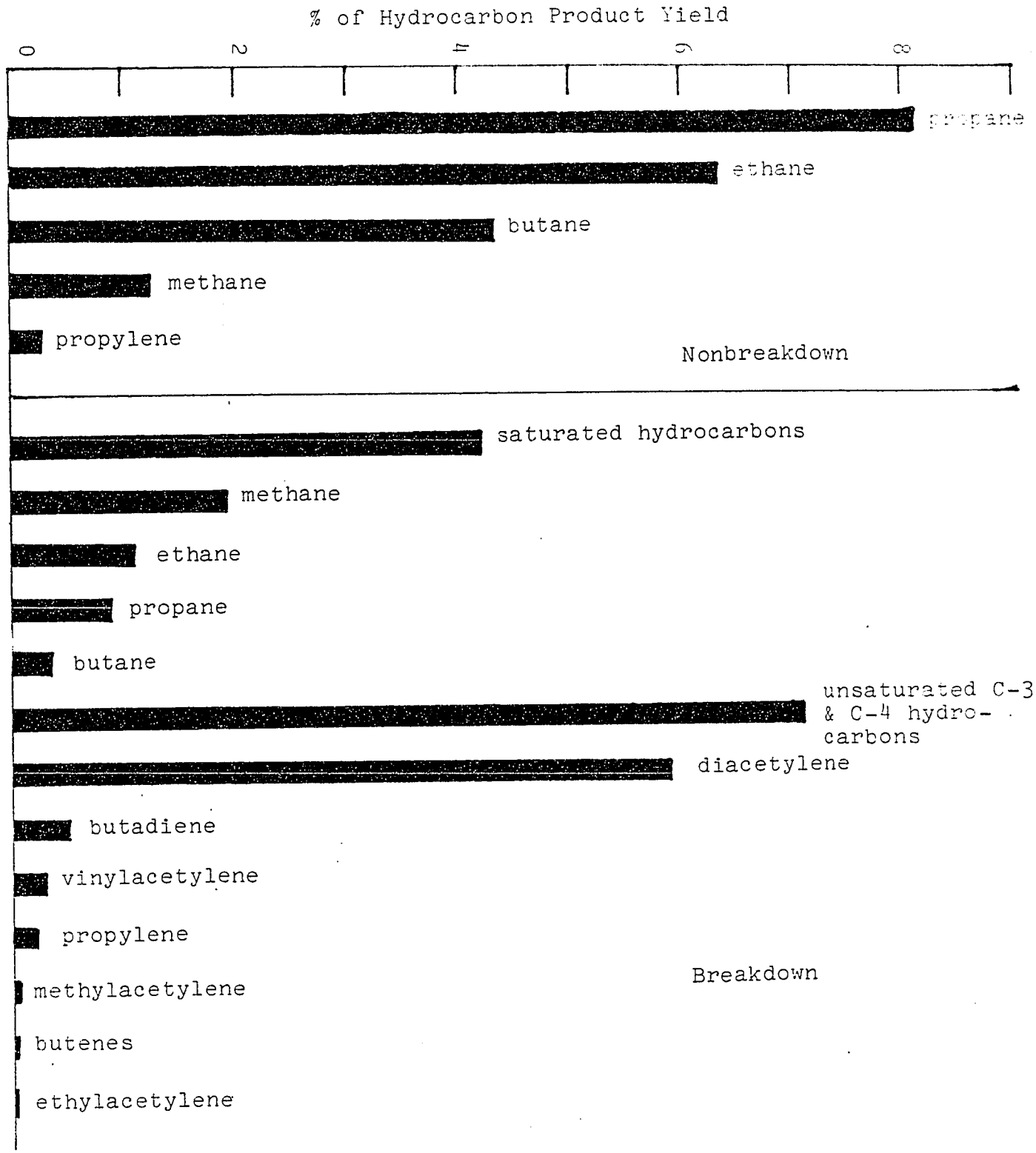

breakdown conditions. Linear plots passing through the origin were obtained for acetylene, methane, ethane, butane, and propylene indicating again a primary origin for these products. For diacetylene, the major unsaturated C-4 hydrocarbon, the upward curvature of the yield-irradiation time plot indicates that this product is secondary. After a long irradiation time (∿100 pulses) a black deposit appeared on the cell windows which caused sparking on the inside of the window surfaces with consequent damage to the windows.

(c) Intensity Dependence of Product Yield

The acetylene yield per pulse as a function of relative intensity is shown in Figure 16(a). Intensity was varied by placing wire gauzes in the path of the beam. Relative intensity is taken as the percent transmittance through the wire gauze as measured by an optoacoustic detector. The gauzes were placed at a sufficient distance from the reaction vessel so that diffraction effects produced by the mesh in the gauze were not important in distorting the energy distribution of the beam. The log-log plot of yield as a function of intensity is linear as shown in Figure 16(b). From the slope of this line, the yield is proportional to intensity to the power 2.3.

The geometrical characteristics of a focussed beam can be the dominant factor affecting the dependence of yield on intensity. If there is a strong dependence of reaction probability on intensity, which is likely for a multiphoton decomposition process, then one can make the following approximation: complete

Figure 13

Product Yield as a Function of Number of Pulses

(Nonbreakdown Conditions)

Laser line: P(26)

Ethylene pressure: 4 torr

■ acetylene

○ propane

▲ ethane

□ butane

● methane

△ propylene

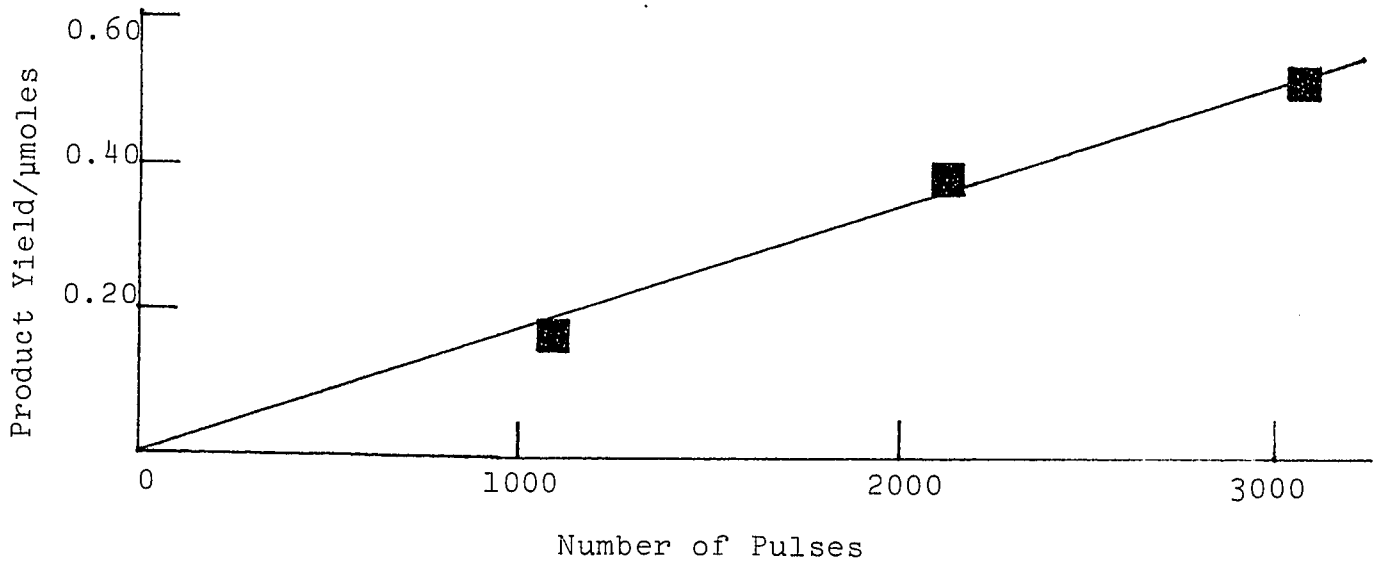
0.60
0.40
0.20
Product Yield/µmoles
0
1000
2000
3000
Number of Pulses

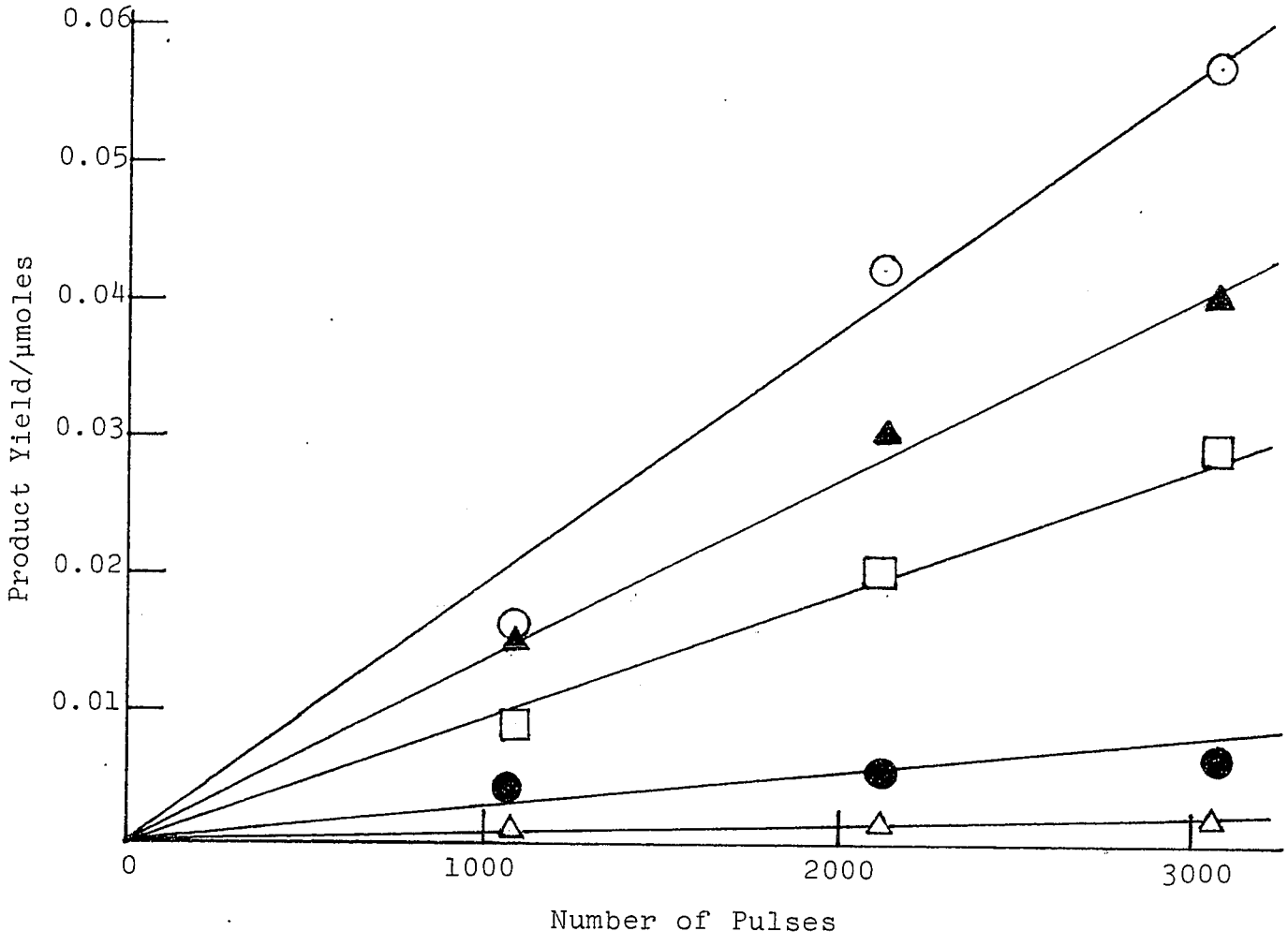
0.06
0.05
0.04
0.03
0.02
0.01
Product Yield/µmoles
0
1000
2000
3000
Number of Pulses

Figure 14

Product Yield as a Function of Number of Pulses

(Breakdown Conditions)

Laser Line: P(26)

Ethylene Pressure: 10 torr

○ methane

▲ ethane

● butane

△ propylene

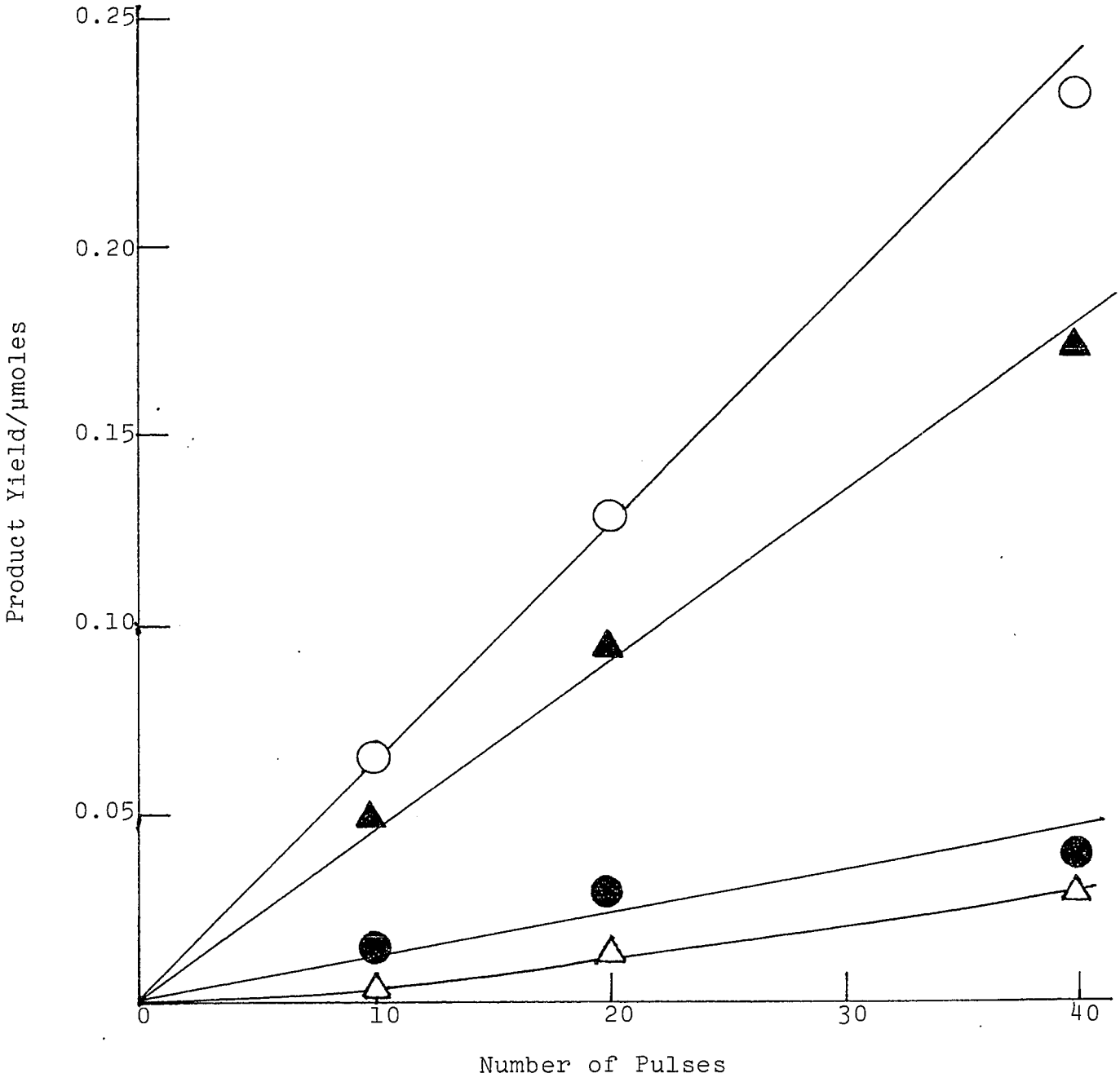
0.25
0.20
0.15
0.10
0.05
Product Yield/µmoles
0
10
20
30
40
Number of Pulses

Figure 15

Product Yield as a Function of Number of Pulses

(Breakdown Conditions)

Laser Line: P(26)

Ethylene Pressure: 10 torr

● acetylene

▲ diacetylene

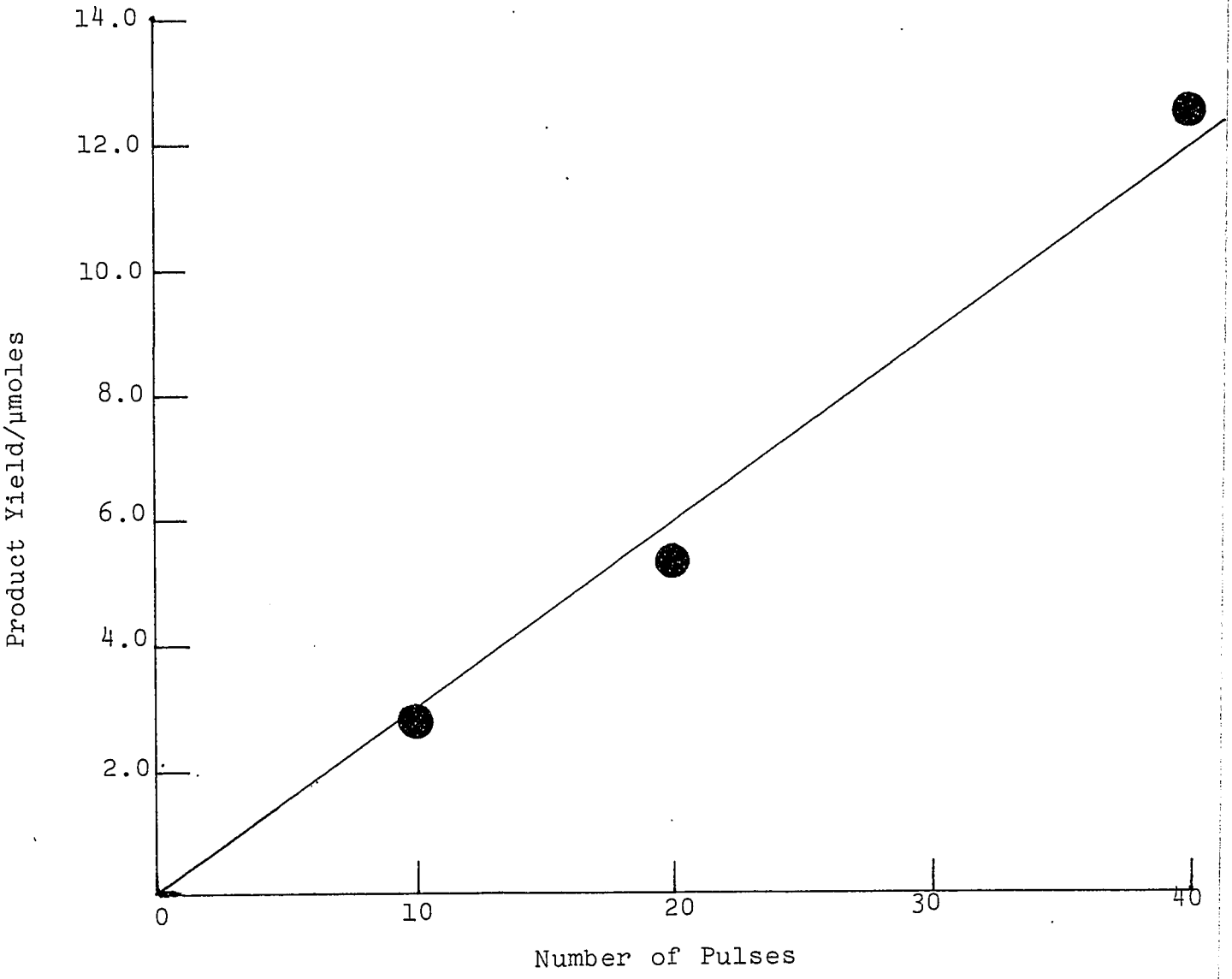
14.0
12.0
10.0
8.0
6.0
4.0
2.0
Product Yield/μmoles
0
10
20
30
40
Number of Pulses

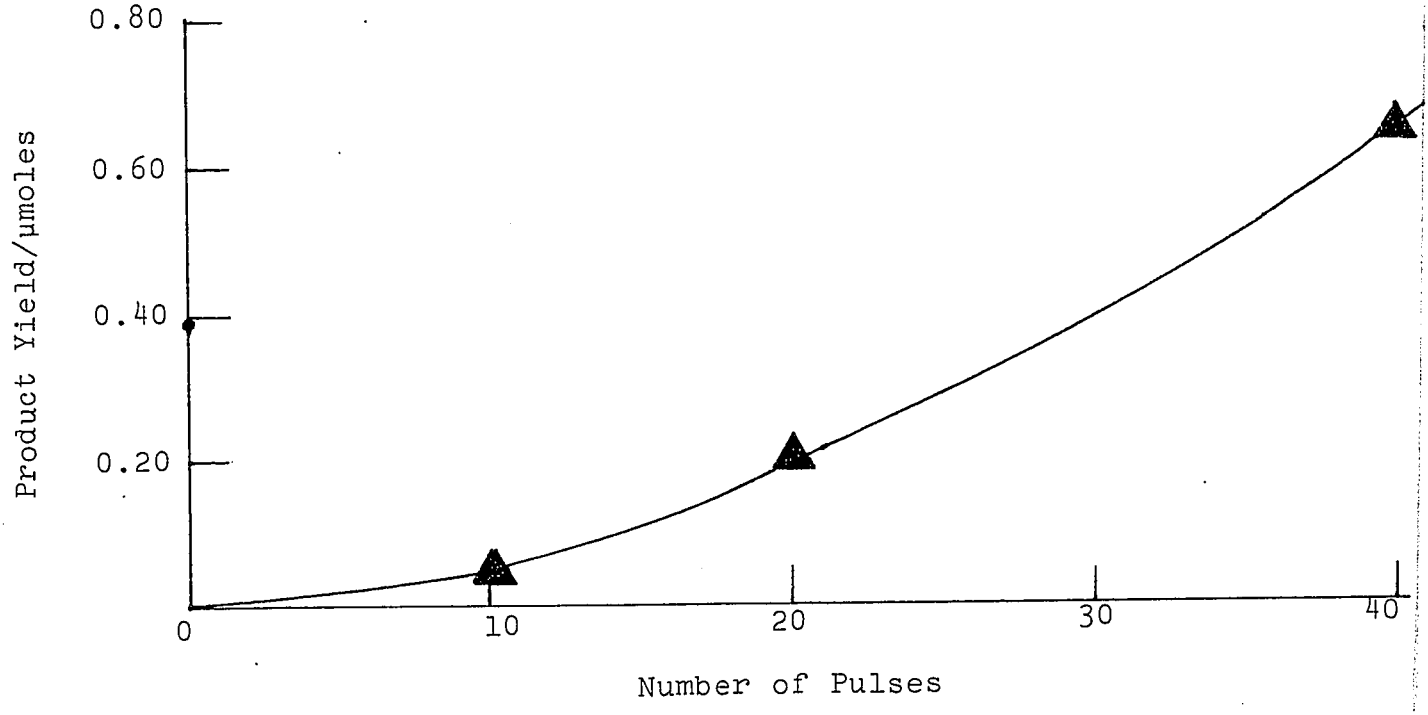
0.80
0.60
0.40
0.20
Product Yield/μmoles
0
10
20
30
40
Number of Pulses

dissociation will take place for virtually all of the molecules within a volume for which the intensity is greater than a threshold value. This "reaction volume" will be saturated by the laser light since no further absorption can occur. Increases in intensity above the threshold value will expand the volume in which saturation takes place. When the intensity is sufficiently high so that most of the reaction occurs outside the small volume of constant beam diameter in the region of the focus (Figure 9), further increases in intensity will merely expand the reaction volume in proportion to the 3/2 power of the incident intensity. The derivation of this scaling law is explained more fully in references 56-58.

The observed power dependence of yield on intensity was somewhat higher than that predicted by the scaling law. This probably means that saturation of absorption of the laser beam was not attained in the volume of reaction for the entire range of intensities studied. In other words, dissociation within the reaction volume was not complete. In the absence of more precise information on the spatial and temporal characteristics of the focussed laser beam, further mechanistic interpretation of the results is not warranted.

(d) Dependence of Product Yield on Pressure

Product yields per pulse as a function of pressure for nonbreakdown conditions are shown in Figure 17. Rather severe constraints were placed on the range of pressure accessible for study. At pressures above 5 torr, optical breakdown was induced. For less than 1 torr, product yields were below the limit of

Figure 16(a)

Acetylene Yield per Pulse as a Function of Relative Intensity

Figure 16(b)

Log (yield per pulse) as a Function of Log (intensity)

(a)

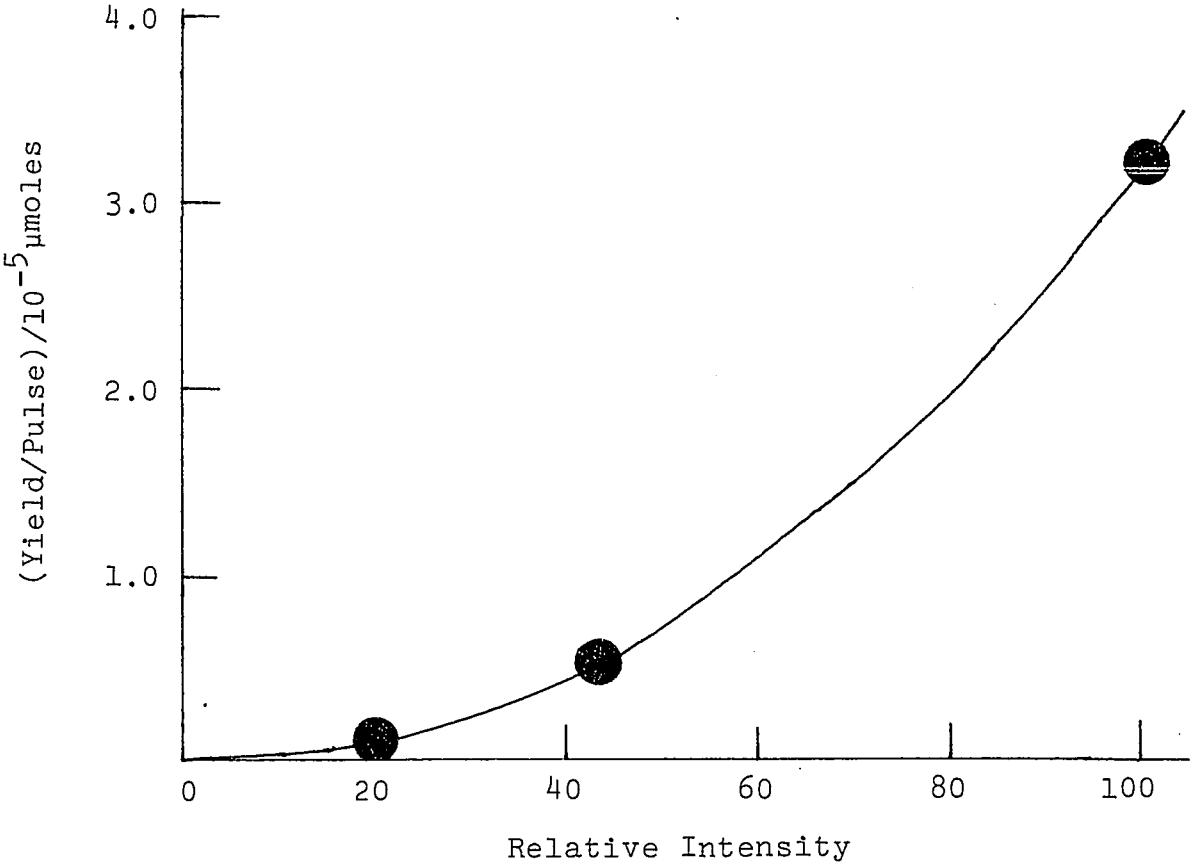
4.0
3.0
2.0
1.0
(Yield/Pulse)/10^{-5} µmoles
0
20
40
60
80
100
Relative Intensity

(b)

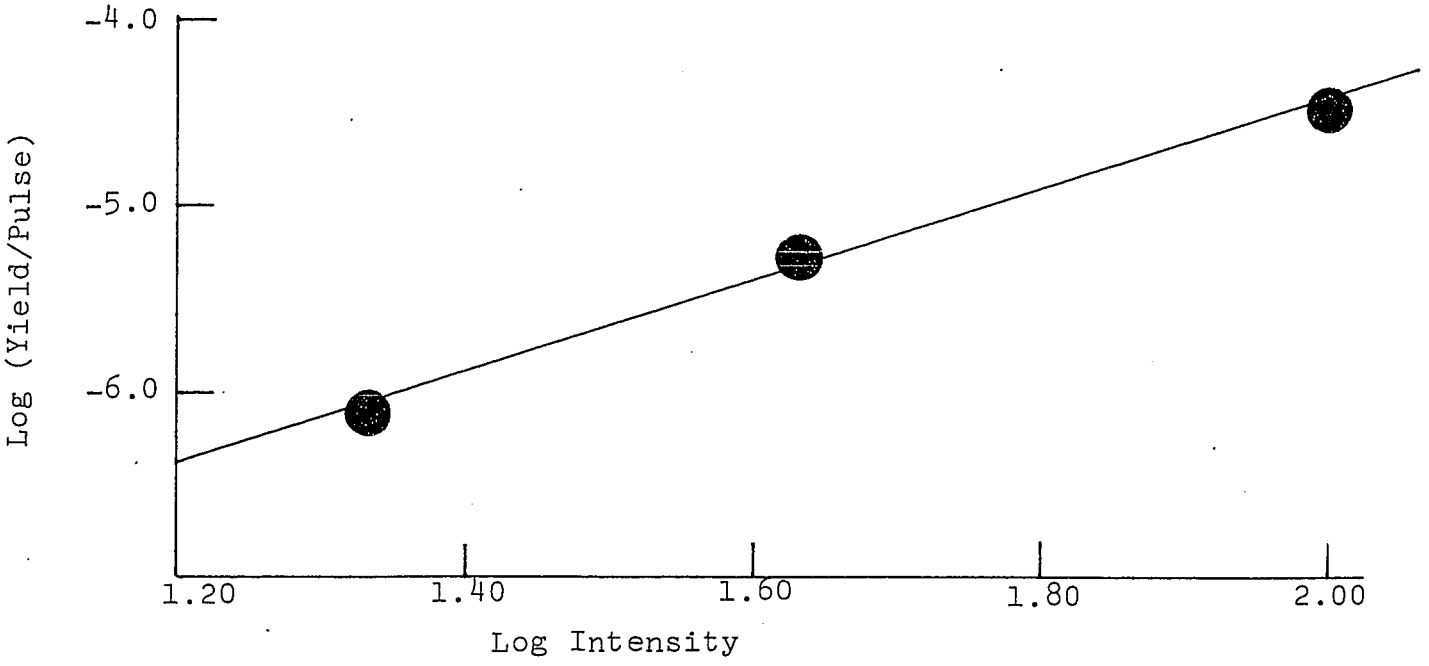
-4.0
-5.0
-6.0
Log (Yield/Pulse)
1.20
1.40
1.60
1.80
2.00
Log Intensity

reliable measurement for reasonable irradiation times. As the pressure decreased from 5 torr to 2 torr, the yields decreased nonlinearly. From 2 torr to 1 torr, the yields were almost independent of pressure. At low intensity, the Beer's law relationship, where absorbance is a linear function of pressure, was observed for ethylene (Figure 8). With the high intensity of the focussed beam, deviations from linear absorbance may occur which could be reflected in the dependence of yield on pressure.

In Figure 18, a linear pressure dependence of the yield is factored out by plotting yield per pulse divided by pressure as a function of pressure. Since this function decreases from 5 to 2 torr, it appears that some process other than linear absorbance of light with pressure was enchancing the reaction at higher pressure. Below 2 torr this function changes its pressure dependency indicating that a change occurred in the reaction process.

The absorption of a large number of photons may be a very fast process. This was experimentally verified by Black et al[59] who observed collisionless multiphoton dissociation of SF_6 using 500 picosecond pulses from a CO_2 laser. The rates of unimolecular dissociations become very rapid after energy in excess of the dissociation energy is acquired.[60] Grant et al[61] demonstrated for the collisionless dissociation of SF_6 in a molecular beam that the time required for the combined absorption and decomposition processes was less than or equal to the laser pulse width of 50 nsec. Some kinetic-molecular theory properties

Figure 17

Yield Per Pulse as a Function of Pressure

- Nonbreakdown Conditions

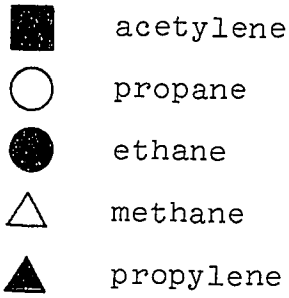

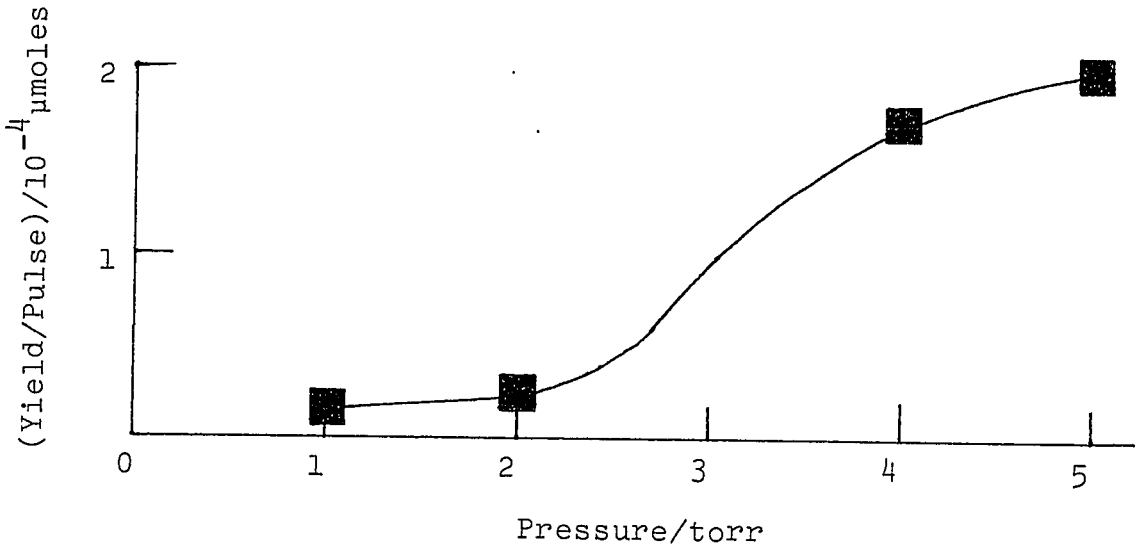
(Yield/Pulse)/10^{-4}µmoles
2
1
0
1
2
3
4
5
Pressure/torr

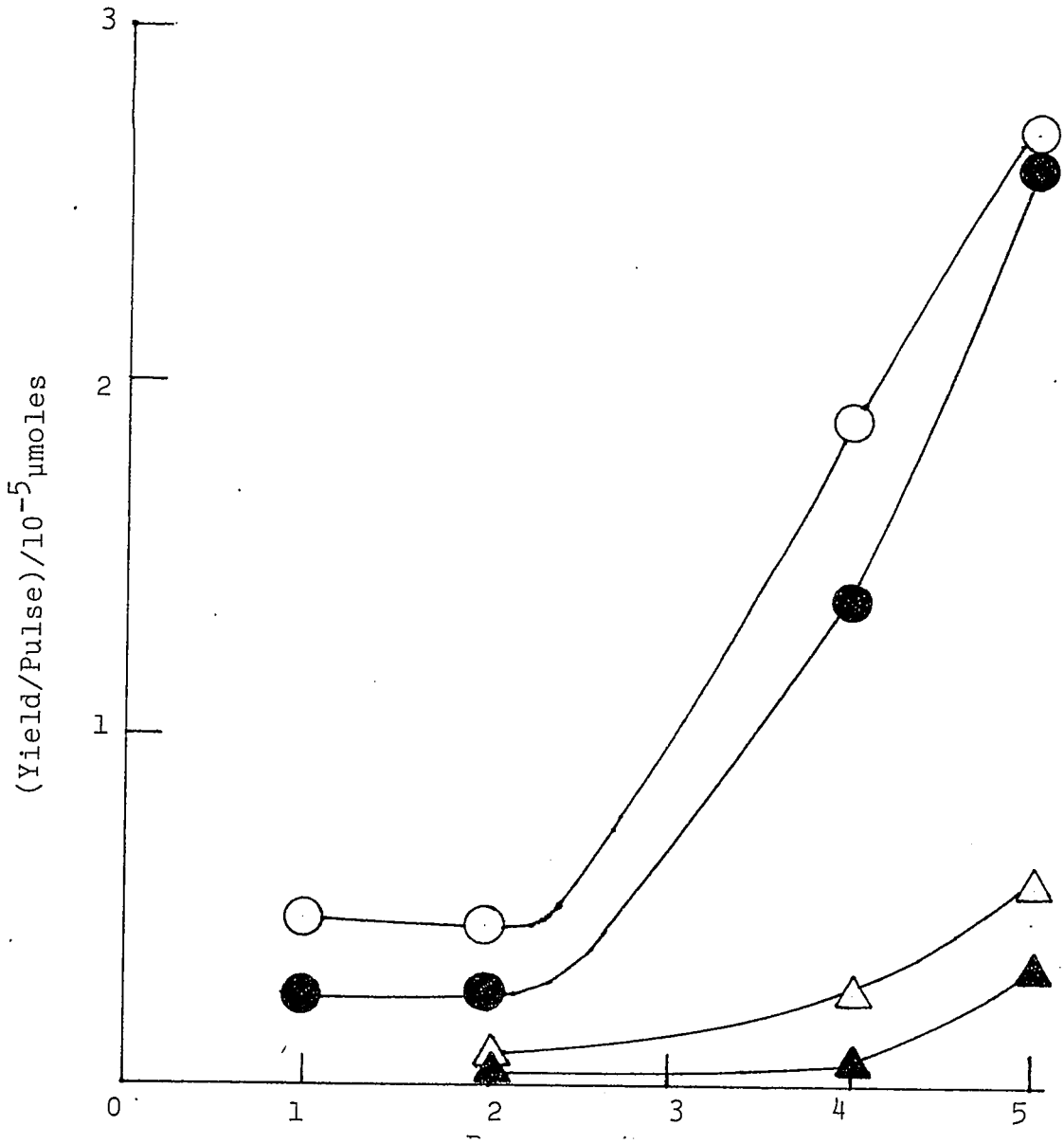
(Yield/Pulse)/10^{-5}µmoles
3
2
1
0
1
2
3
4
5

Figure 18

Yield Per Pulse Divided by Pressure as a Function of Pressure

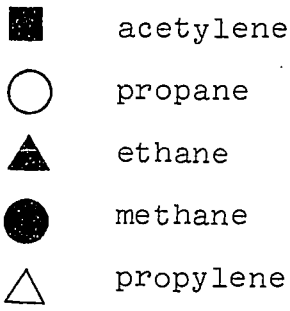

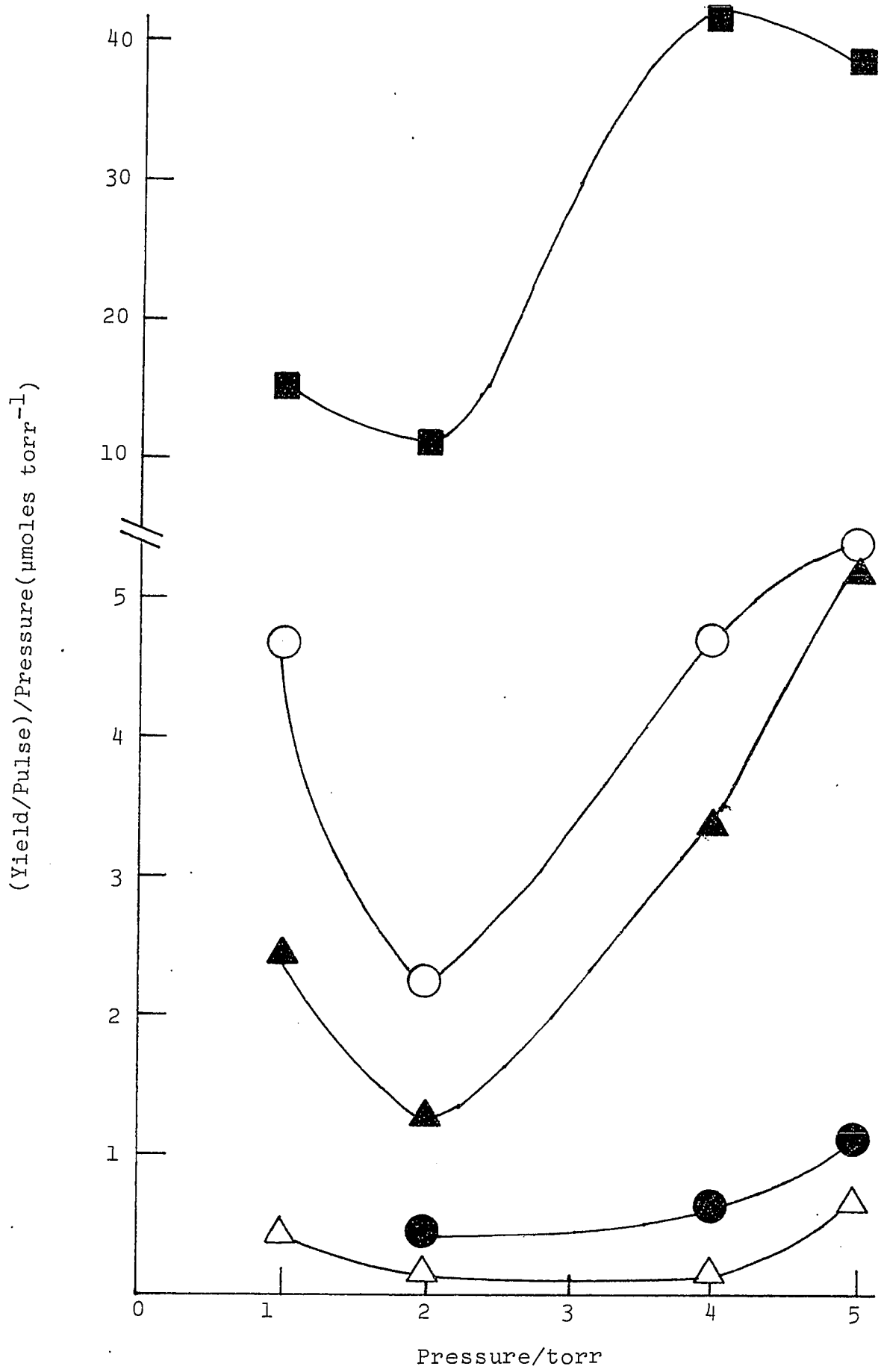
40
30
20
10
5
4
3
2
1
0
1
2
3
4
5
(Yield/Pulse)/Pressure(μmoles torr^{-1})
Pressure/torr

of ethylene are given in Table 4.[62] At low pressure there may be sufficient time before collisional deactivation takes place for molecules to absorb the required number of photons and to have this energy distributed in the proper reaction coordinate for dissociation. The observed dependence of yield on pressure (Figures 17 and 18) suggests that below 2 torr, decomposition via a unimolecular multiphoton process was becoming an effective decomposition channel.

As pressure is increased and collisions become more frequent, collisionless multiphoton dissociation becomes unimportant. The transfer of vibrational energy by collisions is very efficient. For highly energized molecules, collisional transfer of vibrational to rotational and translational degrees of freedom is also likely to be very rapid. Therefore at higher pressures thermalization of the absorbed energy will occur quickly in the reaction zone.

The temperature-time profile in the reaction zone will show a temperature rise as energy becomes thermalized, reach a maximum, and then fall as diffusion processes carry heat away from the reaction zone. The temperature rise will not be strongly dependent on pressure. The rate of diffusion of heat, however, is inversely proportional to pressure and is slow compared to the duration of the laser pulse. As the pressure is raised, the absorbed energy remains for a longer period in the reaction zone and the product yield will increase. The observed rise in product yield from 2 to 5 torr can be interpreted as the result of such a process of diffusion-controlled

Table 4

Kinetic-Molecular Theory Properties of Ethylene at 25°C

Pressure (torr)	Collision Number (collisions/sec)	Average Time Between Collisions (sec)	Mean Free Path (cm)	Collisions Per Laser Pulse
1	1.7×10^{7}	5.9×10^{-8}	2.8×10^{-3}	4
2	3.4×10^{7}	3.0×10^{-8}	1.4×10^{-3}	8
4	6.7×10^{7}	1.5×10^{-8}	7.0×10^{-4}	17
760	1.3×10^{10}	7.8×10^{-11}	3.7×10^{-6}	3200

heat loss from the reaction zone.

Other pressure effects may contribute to the enhancement of yield. Interaction between molecules during collisions changes the electric charge distribution thereby changing the absorption coefficient of a particular vibrational-rotational state for a given wavelength of light. This effect, known as collision broadening, may be a factor in increasing yield at higher pressure as a result of increased absorption of laser light for some of the transitions involved in the dissociation pathway of ethylene.

The "rotational bottleneck effect" has been proposed in some cases to be a limiting factor in absorption of laser light. The very narrow frequency widths of the laser lines used in this work ($\sim$0.1 cm^{-1}) correspond to vibrational transitions for only a few rotational states in the upper and lower levels from among the large number of rotational states populated at room temperature. Fast depletion of the rotational states available for a transition could occur preventing further absorption. As the pressure is increased, repopulation of the depleted rotational states in the lower energy level will be aided by collisions. This would allow absorption to continue without hindrance.

It is not certain whether effects arising from population distribution over rotational states are important in the enhancement of yield with pressure observed from 2 to 5 torr in this study. A limited amount of experimental work done elsewhere suggests that rotational relaxation effects may not

play a part in the enhancement of absorption (see pages 17-18 in Chapter 1).

As the pressure was increased above 5 torr, breakdown was initiated by ionization of the excited molecules[63] and a very rapid reaction rate was observed. Figure 19 shows acetylene yield per pulse as a function of pressure for a series of experiments in a smaller reaction vessel with a shorter focal length lens. Under these conditions the breakdown threshold occurred at a lower pressure. Within experimental error, the plot is linear through the origin. The results are consistent with a mechanism in which dissociation is proportional to light absorbed when absorption follows a Beer's law dependence on pressure.

(e) Hydrogen Yields and Isotopic Studies

A series of experiments was done using the P(14) line with 4 torr pure C_2H_4 in which irradiation time was varied. Figure 20 shows the hydrogen yields as a function of number of laser pulses. The plot is linear and passes through the origin which indicates that hydrogen is a primary product.

Another series of experiments was made irradiating equimolar mixtures of C_2H_4-C_2D_4 at total pressures of 4, 3, and 2 torr with the P(14) line. The hydrogen products as a function of number of pulses are shown in Figures 21-23. The P(14) line is strongly absorbed by C_2H_4 and negligibly absorbed by C_2D_4. (Two torr of pure C_2D_4 were irradiated with 7000 pulses of the P(14) line and no detectable products were obtained).

Figure 19

Acetylene Yield per Pulse as a Function of Pressure-Breakdown Conditions

Cell length: 5 cm

Focal length of lens: 3.0 cm

Laser line: P(26)

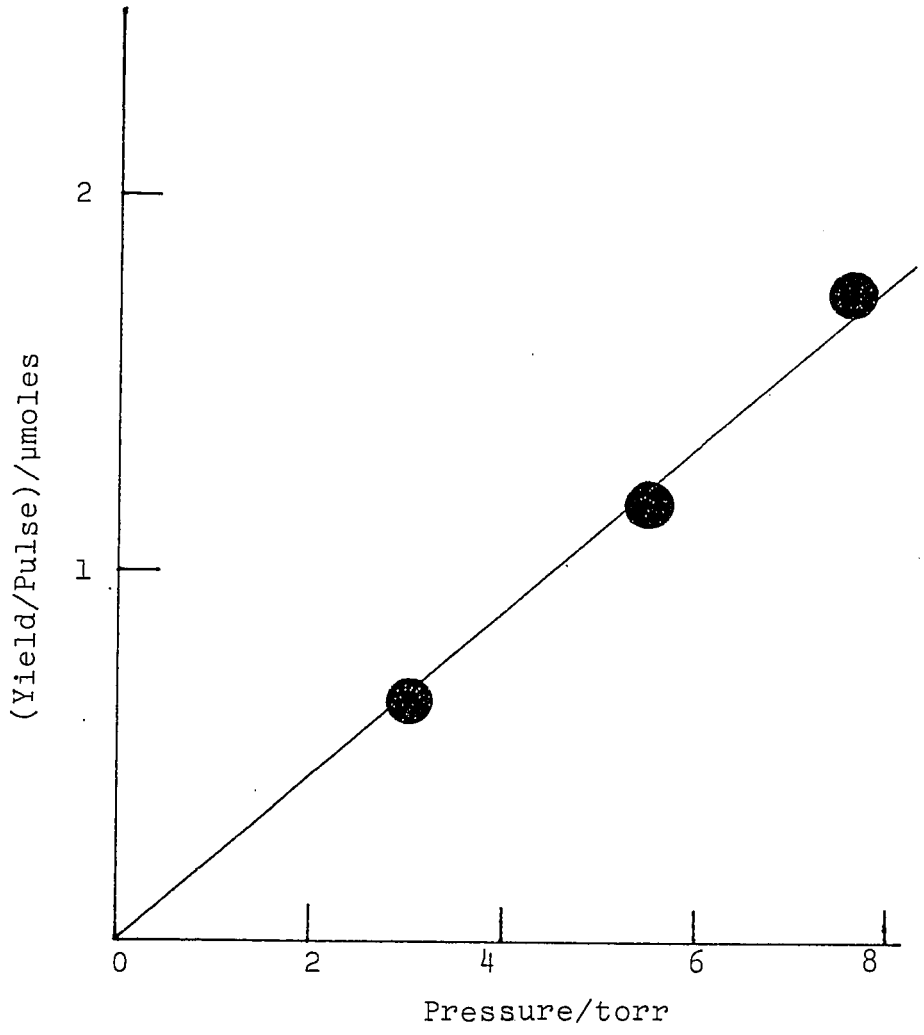
(Yield/Pulse)/μmoles
2
1
0
2
4
6
8
Pressure/torr

Figure 20

Hydrogen Yield as a Function of Number of Laser Pulses

Ethylene pressure: 4 torr

Laser line: P(14)

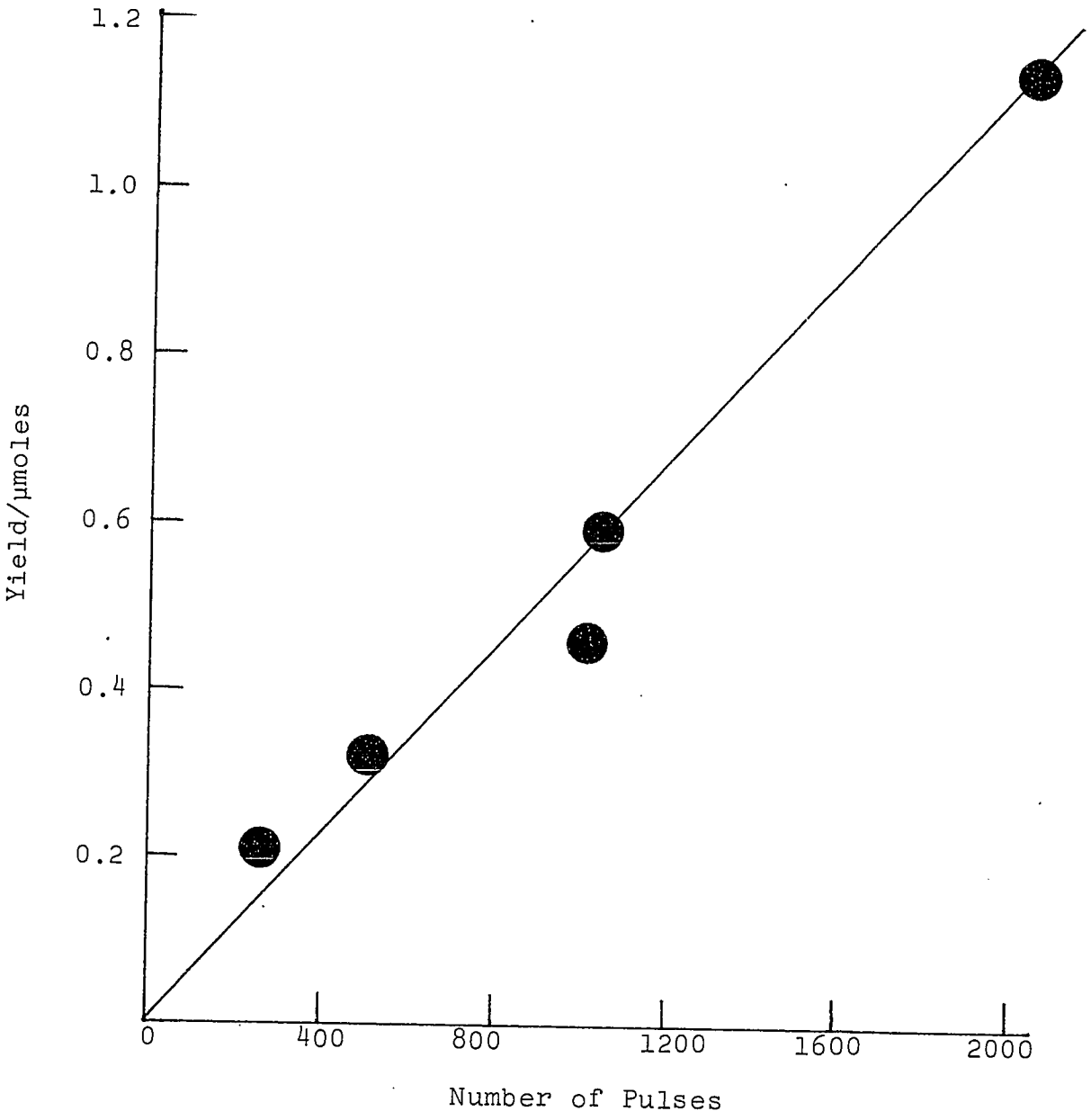
1.2
1.0
0.8
0.6
0.4
0.2
Yield/μmoles
0
400
800
1200
1600
2000
Number of Pulses

As shown in Figure 21, in addition to H_2 significant yields of HD and D_2 were obtained for the mixture of 4 torr total ethylene pressure. The yields of HD were appreciably greater than for D_2. For the mixture of total pressure 3 torr the yield of D_2 was below the limits of detectability (Figure 22), while for the 2 torr mixture (Figure 23) both HD and D_2 were undetectable. For the experiments at 4 torr, the plot of yield as a function of number of pulses (Figure 21) does not extrapolate to the origin. It is believed that this is not a genuine feature of the reaction since it was not observed for 4 torr pure C_2H_4 (Figure 20) or for 3 and 2 torr of the mixture (Figures 22 and 23).

The plots of yield for HD and D_2 for the 4 torr mixture (Figure 21) appear to show some upward curvature indicating a possible secondary source for the formation of these products. Such a source could be the formation of the deuterium-substituted ethylenes C_2H_3D, $C_2H_2D_2$, and C_2HD_3 via exchange of H and D between excited C_2H_4 molecules and C_2D_4. The rate of this exchange is negligible at room temperature.

To investigate this possibility, after separation on a gas chromatographic column, the mass spectrum was taken of the unreacted ethylene from a 4 torr equimolar mixture of C_2H_4-C_2D_4 that had been irradiated with 7215 pulses of the P(14) line. An unirradiated sample of the same mixture was analyzed as a blank. The mass spectra were obtained under low ionization voltages to minimize fragmentation. The results are shown in Table 5.

Figure 21

Hydrogen Products as a Function of Number of Laser Pulses on Irradiation of Equimolar Mixtures of C_2H_4-C_2D_4

Total ethylene pressure: 4 torr

Laser line: P(14)

○ total hydrogen yield

■ H_2

△ HD

● D_2

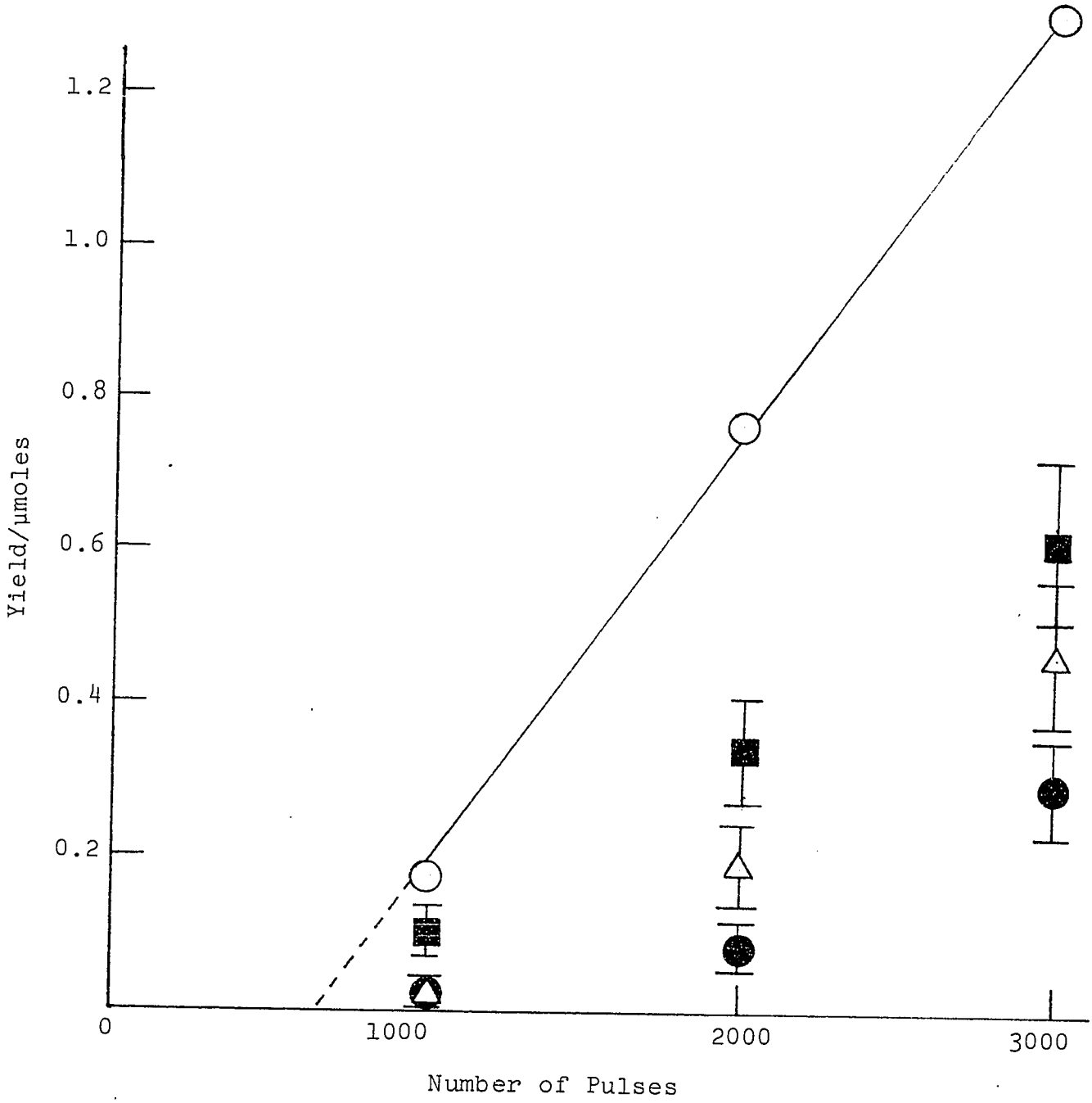
1.2
1.0
0.8
0.6
0.4
0.2
0
Yield/µmoles
1000
2000
3000
Number of Pulses

Figure 22

Hydrogen Products as a Function of Number of Laser Pulses on Irradiation of Equimolar Mixtures of C_2H_4-C_2D_4

Total ethylene pressure: 3 torr

Laser line: P(14)

○ H_2

● HD

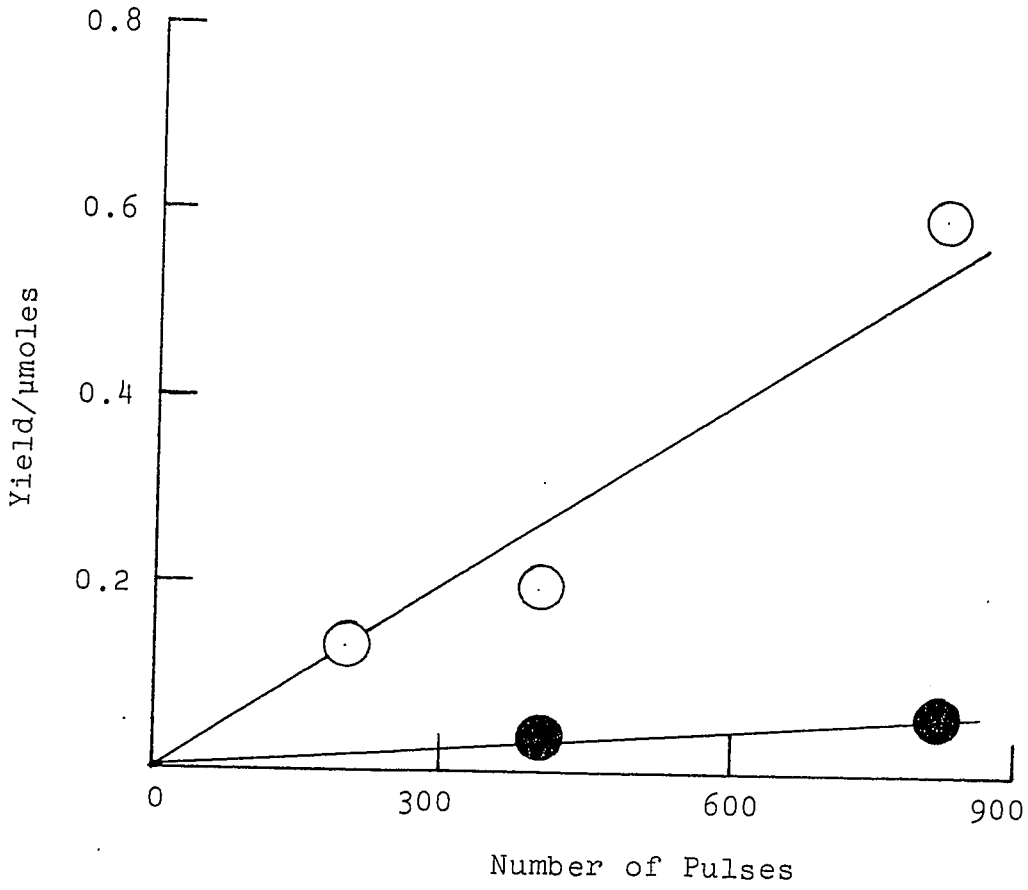
0.8
0.6
0.4
0.2
Yield/μmoles
0
300
600
900
Number of Pulses

Figure 23

Yield of H_2 as a Function of Number of Laser Pulses on Irradiation of Equimolar Mixtures of C_2H_4-C_2D_4

Total ethylene pressure: 2 torr

Laser line: P(14)

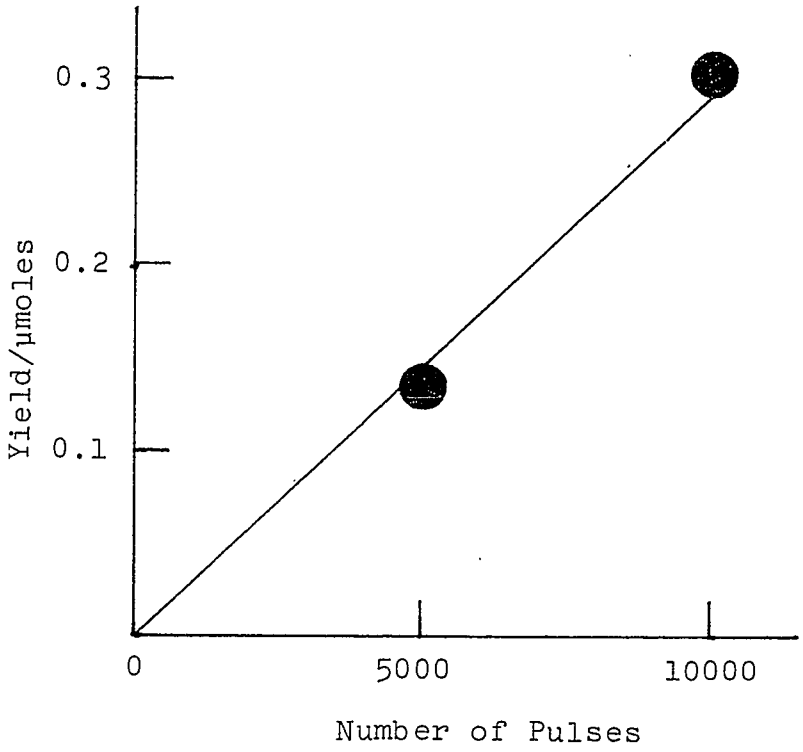
0.3
0.2
0.1
Yield/μmoles
0
5000
10000
Number of Pulses

Table 5

Mass Spectral Study of H-D Exchange

m/e	Relative Abundance			
	Blank	Sample	Δ	
26	8.9	7.6		
27	4.7	3.8		
28	109.5	103.4		
29	2.8	5.0	+2.2	C_2H_3D
30	3.8	2.9	-0.9	$C_2H_2D_2$
31	3.0	5.5	+2.5	C_2HD_3
32	100.0	100.0		
33	2.5	2.5		

ionizing voltage: 10.5 ev

Relative abundances are averaged from 2 scans and corrected for a small background signal of about 1% of the total signal.

The peaks at m/e 26 and 27 and m/e 30 for the blank sample are due to a small amount of fragmentation in the mass spectrometer of C_2H_4 and C_2D_4 respectively. Peaks at m/e 29 and 33 arise from $C^{13}C^{12}H_4$ and $C^{13}C^{12}D_4$. The peak at m/e 31 indicates that C_2HD_3 was present as an impurity to the extent of about 3% of the C_2D_4. However, since the absorption coefficient of C_2HD_3 is much smaller than that of C_2H_4 at 949.5 cm^{-1} [64], this impurity is not likely to be a significant source of HD product. C_2H_3D and asymmetric-$C_2H_2D_2$ do have strong absorption bands in the region of the P(14) laser line[65].

The mass spectrum for the irradiated sample shows no increase for the peak at m/e 30. This indicates the absence of $C_2H_2D_2$ which might have been formed through a cyclobutane intermediate:

$$C_2H_4 + C_2D_4 \rightarrow \begin{matrix} H_2C\cdots CH_2 \\ \vdots \quad \vdots \\ D_2C\cdots CD_2 \end{matrix} \rightarrow C_2H_2D_2 + C_2H_2D_2$$

Increases of about 2.5% each were noted in the relative abundances of the peaks at m/e 29 and 31 corresponding to formation of C_2H_3D and C_2HD_3. The exchange mechanism could be:

$$H + C_2D_4 \rightarrow D + C_2HD_3$$

$$D + C_2H_4 \rightarrow H + C_2H_3D$$

and

$$C_2H_3 + C_2D_4 \rightarrow C_2H_3D + C_2D_3$$

$$C_2D_3 + C_2H_4 \rightarrow C_2HD_3 + C_2H_3$$

where hydrogen atoms or vinyl radicals originate from dissociation of excited ethylene.

Assuming that deuterium-substituted ethylenes are no more likely to react than C_2H_4, the results indicate that hydrogen-deuterium exchange occurred to the extent of no more than 5% of the reactant molecules. The observed HD/H_2 product ratios are large in comparison to the proportion of deuterium-substituted ethylenes formed in the exchange process. Therefore most of the HD must have been formed directly from the original C_2H_4 and C_2D_4 in the reactant mixture, not from photolysis of deuterium-substituted ethylenes. This shows that a radical mechanism is an important primary process in the laser-induced decomposition of ethylene.

A measure of the isotopic selectivity of a process is the separation factor α defined as $(M/M')\div(M_o/M_o')$ where M and M' are the amounts of the isotopic species M and M' found in the products, and M_o and M_o' are the amounts of species M and M' originally present in the reactants. In this work M and M' are H and D and the products of interest are H_2, HD, and D_2. For the equimolar C_2H_4-C_2D_4 reactant mixtures $M_o = M_o'$ so that α is given by the ratio H/D for the hydrogen products. Mean α values for the 4, 3, and 2 torr mixtures were calculated to be 2.4, 3.9, and 5.1 respectively. In the cases where HD or D_2 were undetectable, the yields were assumed to be equal to the limit of detectability. Thus for the 3 and 2 torr mixtures the α values stated are minima and may actually have been considerably greater.

The decrease in α values as pressure is raised reflect a loss of isotopic selectivity due to collisional energy transfer

from C_2H_4 molecules to C_2D_4. The greater frequency of collisions accompanying an increase in pressure enables a larger number of C_2D_4 molecules to reach the energized state from which dissociation occurs.

An attempt was made to dissociate C_2D_4 using the focussed R(22) laser line at 1080 cm^{-1}. This is the frequency of maximum "linear" absorption for the spectral range of the CO_2 laser. Irradiation of 2 torr of pure C_2D_4 with 7000 pulses produced no detectable products. This appears to result from a smaller absorption coefficient than for the frequencies used to excite C_2H_4.

VII. Reaction Mechanism

(a) Nonbreakdown Conditions

A reaction scheme which plausibly explains the product distribution under nonbreakdown conditions is:

$$C_2H_4^* \rightarrow C_2H_2 + H_2 \quad (1)$$

$$C_2H_4^* \rightarrow C_2H_3^* + H \quad (2)$$

$$C_2H_4^* + M \rightarrow C_2H_4 + M \quad (3)$$

$$C_2H_3^* \rightarrow C_2H_2 + H \quad (4)$$

$$C_2H_3^* + M \rightarrow C_2H_3 + M \quad (5)$$

$$H + C_2H_4 \begin{cases} \rightleftarrows C_2H_5 & (6) \\ \rightarrow C_2H_3 + H_2 & (7) \end{cases}$$

$$2C_2H_5 \begin{cases} \rightarrow C_4H_{10} & (8) \\ \rightarrow C_2H_4 + C_2H_6 & (9) \end{cases}$$

$$H + C_2H_5 \rightleftarrows C_2H_6^* \quad (10)$$

$$C_2H_6^* \rightarrow 2CH_3 \qquad (11)$$

$$C_2H_6^* + M \rightarrow C_2H_6 + M \qquad (12)$$

$$2CH_3 \rightarrow C_2H_6 \qquad (13)$$

$$CH_3 + C_2H_5 \begin{cases} \rightarrow C_3H_8 & (14) \\ \rightarrow C_2H_4 + CH_4 & (15) \end{cases}$$

$$CH_3 + C_2H_3 \rightarrow C_3H_6 \qquad (16)$$

The products from the nonbreakdown reaction differ considerably from those of the low temperature thermal pyrolysis (500-600°C) where no hydrogen or acetylene are formed. On the other hand, pyrolysis at high temperatures (1200-1900°C) using shock tubes produces hydrogen and acetylene as major products, but no significant amount of saturated hydrocarbons. In a flow pyrolysis study of ethylene diluted in nitrogen for the intermediate temperature range 730-1330°C[66], the major primary products were: H_2(37%), C_4H_6(25%), C_2H_2(8%), C_3H_6(8%), C_2H_6(6%), and C_3H_8(6%). This more nearly resembles the products found in the present study but still shows major differences.

The product distribution obtained for nonbreakdown conditions is very similar to that found for ultraviolet flash photolysis[29]. An analogous mechanism to steps (2) to (15) in the Introduction (Section IV (c)) probably applies for this study. Acetylene can be formed both by the molecular process (1) and the radical sequence of steps (2) and (4). Butane and ethane are produced by combination (8) and disproportionation (9) of ethyl radicals.

Both the laser and flash photolyses have the common feature of a high concentration of radicals produced during a

short time interval. This situation is favorable for the hydrogen atom "cracking" process (10), (11) which leads to significant production of ethane, propane, methane, and propylene by steps (13)-(16). At higher pressure, de-energization of the excited ethane molecule (12) can take place before decomposition has a chance to occur. The consequent reduction in methyl radical formation results in diminishing relative importance of propane, methane, and propylene which was observed in this study as the pressure was increased.

However, differences must exist between the mechanisms for the nonbreakdown laser photolysis and ultraviolet photolysis. This is apparent from ultraviolet photolysis studies[27] where irradiation of mixtures of C_2H_4-C_2D_4 gave very little HD. Therefore hydrogen resulted almost entirely from the molecular process (1). In contrast, the significant yields of HD in this study show that a free atom precursor exists as an important source of hydrogen. HD must have come from abstraction processes such as

$$H + C_2D_4 \rightarrow C_2D_3 + HD$$
$$D + C_2H_4 \rightarrow C_2H_3 + HD$$

Therefore it is necessary to include step (7) in the reaction mechanism. It appears that the higher temperature produced in the laser photolysis enables hydrogen atom abstraction (7) to compete with addition (6).

Isotopic selectivity for the radical process is reduced because hydrogen atoms may abstract from either deuterated or nondeuterated ethylene. The significant degree of selectivity

achieved in the isotope studies indicates that production of hydrogen by a molecular process is probably important in the reaction mechanism.

The observation that saturated hydrocarbons became more important as the pressure was lowered indicates that the radical process increases in relative importance compared to the molecular process (1) at lower pressure. Activation energies for processes (1) and (2) were determined from shock tube work[25] to be around 79 and 98 kcal/mole respectively. Unimolecular reaction (2) is probably favored at low pressure because ethylene has more time before collisional deactivation occurs to absorb the greater number of photons and attain the more highly energized activated state required for the radical split.

Consideration can be given to participation of a bimolecular initiation process as was suggested in the low temperature pyrolysis:

$$C_2H_4^* + C_2H_4 \rightarrow C_2H_3 + C_2H_5 \qquad (17)$$

Since the temperature of the irradiation zone is ill-defined and the orders of the unimolecular initiation steps (1) and (2) are not known, it is not feasible to assess the relative importance of the bimolecular and unimolecular processes by determination of rate expressions using the kinetic characteristics of the reaction. However, the fact that isotopic selectivity was maintained indicates that the unimolecular processes were dominant. The bimolecular process (17) is not likely to give rise to isotopic selectivity in reaction products. Also, the

increasing importance of saturated hydrocarbons as the pressure was lowered is more consistent with the unimolecular step (2) rather than the bimolecular step (17) being the dominant radical initiation process.

Additional hydrogen and acetylene may have arisen from the process

$$H + C_2H_3 \rightarrow C_2H_2 + H_2 \qquad (18)$$

A certain amount of saturated hydrocarbons may also have been formed by the processes (19)-(25):

$$CH_3 + C_2H_4 \begin{cases} \rightarrow C_2H_3 + CH_4 & (19) \\ \rightarrow C_3H_7 & (20) \end{cases}$$

$$C_3H_7 + H \rightarrow C_3H_8 \qquad (21)$$

$$C_2H_5 + C_2H_4 \begin{cases} \rightarrow C_2H_3 + C_2H_6 & (22) \\ \rightarrow C_4H_9 & (23) \end{cases}$$

$$C_4H_9 + H \rightarrow C_4H_{10} \qquad (24)$$

$$CH_3 + H + M \rightarrow CH_4 + M \qquad (25)$$

(b) Breakdown Conditions

A number of unsaturated hydrocarbons were formed under breakdown conditions which were absent under nonbreakdown conditions. It is likely that these are secondary products formed from decomposition of the primary product acetylene under the high temperature conditions in the laser-induced plasma. Supportive evidence comes from studies of shock tube decomposition of acetylene where diacetylene, vinylacetylene, and butadiene have been observed as the major products[67,68,69].

As suggested by Just et al[25] for the shock tube pyrolysis of ethylene, a plausible pathway for formation of the major secondary product diacetylene is

$$H + C_2H_2 \rightarrow C_2H + H_2$$
$$C_2H + C_2H_2 \rightarrow C_4H_2 + H \ .$$

Isotope studies were not made for the decomposition involving breakdown. Isotopic selectivity would not be expected because of the high concentration of fragments in the laser-induced plasma which will react randomly.

VIII. Limitations to the Present Study and Suggestions for Further Work

Limitations were placed on the pressure and intensity ranges available in this study. At pressures of 5 torr and above, optical breakdown was induced. At less than 1 torr, product yields were below the limits of detectability of the analytical instruments for reasonable irradiation times. Variations in intensity by changing the focal length of the lens were not feasible because the use of longer or shorter focal length lenses would cause damage to the cell windows. The focal cone of the beam must be almost entirely within the reaction vessel because the threshold for damage to sodium chloride or germanium is exceeded for laser radiation of moderate intensity produced in a beam that is only slightly focussed. Further studies could extend the range to some extent by the use of a longer reaction vessel in combination with a longer focal length lens. The

increased path length could compensate for the lower intensity in the focal region allowing measurable product yields to be obtained. Further work might also be done to examine the product dependence on frequency by using other laser lines.

The primary limitation of the infrared laser-induced dissociation of ethylene is the low yields. These appear insufficient to make ethylene a practical source for isotope enrichment. Nevertheless, further studies to examine the isotope selectivity of the acetylene products would be useful. Even though nonselective radical processes play an important role in the decomposition, isotopic selectivity for formation of acetylene may be retained to a high degree. This is possible since acetylene from processes (1) and (4) can be formed directly from a selectively excited ethylene molecule.

Claims to Original Research

1. The first detailed study of product distribution from infrared laser photolysis of ethylene has been achieved.
2. Evidence for a transition in reaction mechanism from a collisionless multiphoton process at low pressure to a diffusion-controlled high temperature thermolysis at high pressure has been obtained.
3. A sharp pressure threshold exists for a given intensity in the focussed beam above which optical breakdown occurs accompanied by visible luminescence.
4. Below the breakdown threshold, the results indicate the participation of both molecular and radical processes in the reaction.
5. A striking similarity in the product distribution to that for ultraviolet flash photolysis has been observed. A reaction scheme which bears many analogous features to this process has been discussed for the laser-induced photolysis.
6. Photolysis of ethylene in C_2H_4-C_2D_4 mixtures showed that some isotopic selectivity in the reaction products was achieved.

References

1. B.A. Lengyel; Lasers, 2nd ed., Wiley-Interscience, New York (1971).
2. M. Garbuny; "Tunable Infrared Lasers" in Laser Photochemistry; Tunable Lasers and Other Topics, Physics of Quantum Electronics, Vol. 4; S.F. Jacobs, M. Sargent, M.O. Scully, C.T. Walker, ed. Addison-Welsey (1976).
3. J.J. Ewing; Physics Today, 31, 32 (1978).
4. J.P. Aldridge, J.H. Birely, C.D. Cantrell, D.C. Cartwright; "Studies of Laser Isotope Separation", op. cit. ref. 2.
5. V.S. Letokhov; "Principles of Laser Isotope Separation" in Frontiers in Laser Spectroscopy, Vol. 2; Balian, Haroche, and Liberman, ed. (1977).
6. C.D. Cantrell, S.M. Freund, J.L. Lyman; "Laser Induced Chemical Reactions and Isotope Separation" in Laser Handbook Vol. 3(b); M.L. Stitch, ed., North-Holland, New York (1978).
7. W.M. Shaub, S.H. Bauer; Int. J. Chem. Kinetics 7, 509 (1975).
8. S.H. Bauer; Chem. Rev. 78, 147 (1978).
9. N.R. Isenor, M.C. Richardson; Appl. Phys. Lett. 18, 224 (1971).
10. R.V. Ambartzumian, V.S. Letokhov, E.A. Ryabov, N.V. Chekalin; JETP Lett. 20, 273 (1974).
11. S. Kimel, S. Speiser; Chem. Rev. 77, 437 (1977).
12. R.V. Ambartzumian, N.P. Furzikov, Y.A. Gorokhov, V.S. Letokhov, G.N. Makarov, A.A. Puretzky; JETP Lett. 23, 217 (1976).
13. R.V. Ambartzumian, V.S. Letokhov; Acc. Chem. Res. 10, 61 (1977).
14. N. Bloembergen, E. Yablonovitch; Physics Today, 31, 23 (1978).
15. C.G. Silcocks; Proc. Roy. Soc. London, Ser. A 233, 465 (1956).

16. G. Dahlgren, J.E. Douglas; J. Am. Chem. Soc. 80, 5108 (1958).

17. M. Taniewski; Proc. Roy. Soc. London, Ser. A 265, 519 (1962).

18. M.P. Halstead, C.P. Quinn; Trans. Faraday Soc. 64, 103 (1968).

19. M.L. Boyd, T.M. Wu, M.H. Back; Can. J. Chem. 46, 2415 (1968).

20. M. Simon, M.H. Back; Can. J. Chem. 47, 251 (1969).

21. G.B. Skinner, E.M. Sokoloski; J. Phys. Chem. 64, 1028 (1960).

22. I.D. Gay, R.D. Kern, G.B. Kistiakowsky, H. Niki; J. Chem. Phys. 45, 2371 (1966).

23. J.B. Homer, G.B. Kistiakowsky; J. Chem. Phys. 47, 5290 (1967).

24. G.B. Skinner, R.C. Sweet, S.K. Davis; J. Phys. Chem. 75, 1 (1971).

25. T. Just, P. Roth, R. Damm in Proceedings of 16th International Symposium on Combustion pp. 961-969 (1976).

26. M.C. Sauer, L.M. Dorfman; J. Chem. Phys. 35, 497 (1961).

27. H. Okabe, J.R. McNesby; J. Chem. Phys. 36, 601 (1962).

28. E. Tschuikow-Roux, J.R. McNesby, W.M. Jackson, J.L. Faris; J. Phys. Chem. 71, 1531 (1967).

29. R.A. Back, D.W.L. Griffiths; J. Chem. Phys. 46, 4839 (1967).

30. R. Gorden, P. Ausloos; J. Chem. Phys. 47, 1799 (1967).

31. Y. Inel, A. Siddiqui, G.G. Meisels; J. Phys. Chem. 75, 1317 (1971).

32. P. Potzinger, L.C. Glasgow, G. von Bunau; Z. Naturforsch. A 27, 628 (1972).

33. H. Hiroshi, K. Kodama, I. Tanaka; Bull. Chem. Soc. Japan 48, 711 (1975).

34. G.G. Meisels; Advan. Chem. Ser. 58, 243 (1966).

35. K.J. Laidler, L.F. Loucks in Comprehensive Chemical Kinetics Vol. 5, Ch. 1, C.H. Bamford, C.F. Tipper, ed. Elsevier (1972).

36. R. Miquel, J. Drillat, J. Bonnet; Bull. Soc. Chim. France, 271 (1969).

37. K.L. Paciorek, R.H. Kratzer; Can. J. Chem. 48, 1777 (1970).

38. M. Takeuchi, Y. Takezaki; Bull. Inst. Chem. Res., Kyoto Univ. 49, 230 (1971).

39. S.I. Ivanov; Bulg. J. Phys. 4, 427 (1976).

40. J. Itoh, K. Takimoto, S. Tsuda; Bull. Chem. Soc. Japan 50, 2183 (1977).

41. J.P. Bell, R.V. Edwards, B.R. Nott, J.C. Angus; I & EC Fundamentals 13, 89 (1974).

42. J.W. Robinson, P.J. Moses, P.M. Boyd; Spec. Lett. 7, 395 (1974).

43. J. Tardieu de Maleissye, F. Lempereur, C. Marsal; Chem. Phys. Lett. 42, 472 (1976).

44. R.V. Ambartzumian, N.V. Chekalin, V.S. Letokhov, E.A. Ryabov; Chem. Phys. Lett. 36, 301 (1975).

45. N.V. Chekalin, V.S. Dolzhikov, V.S. Letokhov, V.N. Lokhman, A.N. Shibanov; Appl. Phys. 12, 191 (1977).

46. V.N. Bagratashvili, I.N. Knyazev, V.S. Letokhov, V.V. Lobko; Opt. Comm. 18, 525 (1976).

47. V.N. Bagratashvili, I.N. Knyazev, V.S. Letokhov, V.V. Lobko; Opt. Comm. 14, 426 (1975).

48. O.N. Avatkov, V.N. Bagratashvili, I.N. Knyazev, Y.R. Kolomiisky, V.S. Letokhov, V.V. Lobko, E.A. Ryabov; Sov. J. Quantum Electronics 7, 412 (1977).

49. S.S. Alimpiev, V.N. Bagratashvili, N.V. Karlov, V.S. Letokhov, V.V. Lobko, A.A. Makarov, B.G. Sartakov, E.M. Khoklov; JETP Lett. 25, 547 (1977).

50. A.S. Akhmanov, V.Y. Baronov, V.D. Pismenny, V.N. Bagratashvili, Y.R. Kolomiisky, V.S. Letokhov, E.A. Ryabov; Opt. Comm. 23, 357 (1977).

51. J. Bastiaens, D. deKeuster, X. de Hemptinne; Bull. Soc. Chim. Belg. 85, 833 (1976).

52. N.C. Peterson, R.G. Manning, W. Braun; to be published.

53. A. Yariv; Quantum Electronics, J. Wiley & Sons (1976).

54. H. Weichel, L.S. Pedrotti; Electro-Optical Systems Design 8, 34 (1976).

55. Selected Values of Physical and Thermodynamic Properties of Hydrocarbons and Related Compounds, American Petroleum Institute (1953).

56. S. Speiser, J. Jortner; Chem. Phys. Lett. 44, 399 (1976).

57. D.R. Keefer, J.E. Allen; Chem. Phys. Lett. 43, 394 (1976).

58. W. Fuss, T.P. Cotter; Appl. Phys. 12, 265 (1977).

59. J.G. Black, E. Yablonovitch, N. Bloembergen, S. Mukamel; Phys. Rev. Lett. 38, 1131 (1977).

60. P.J. Robinson, K.A. Holbrook, Unimolecular Reactions, J. Wiley (1972).

61. E.R. Grant, M.J. Coggiola, Y.T. Lee, P.A. Schultz, A.S. Sudbo, Y.R. Shen; Chem. Phys. Lett. 52, 595 (1977).

62. G.M. Barrow, Physical Chemistry, Ch. 2, McGraw-Hill, 3rd ed. (1973).

63. D.C. Smith, R.G. Meyerand, "Laser Radiation-Induced Gas Breakdown" in Principles of Laser Plasmas, J. Wiley & Sons (1976).

64. J. Charette, M. de Hemptinne; Bull. Acadamie Royale de Belgique 37, 436 (1951).

65. B.L. Crawford, J.E. Lancaster, R.G. Inskeep; J. Chem. Phys. 21, 678 (1952).

66. G.D. Towell, J.J. Martin; Am. Inst. Chem. Eng. Journal 7, 693 (1961).

67. E.F. Greene, R.L. Taylor, W.L. Patterson; J. Phys. Chem. 62, 238 (1958).

68. G.B. Skinner, E.M. Sokoloski; J. Phys. Chem. 64, 1952 (1960).

69. I.D. Gay, G.B. Kistiakowsky, J.V. Michael, H. Niki; J. Chem. Phys. 43, 1728 (1965).

Appendix 1: Mass Spectral Identification of Products

lit - literature value for relative abundance of peak at given mass to charge ratio (m/e), from Compilation of Mass Spectral Data; A. Cornu, R. Massot; Heyden & Son (1966).

exp - experimentally observed value for relative abundance of peak at given m/e

ethane	m/e	26	27	29	30				
	lit	23	33	22	26				
	exp	29	33	27	27				
propane	m/e	29	39	41	43				
	lit	100	17	15	34				
	exp	100	32	26	64				
acetylene	m/e	12	13	24	25	26	27		
	lit	2	6	6	20	100	3		
	exp	2	5	9	32	100	3		
propylene	m/e	39	41	42					
	lit	71	100	68					
	exp	40	100	60					
methylacetylene	m/e	38	39						
	lit	29	79						
	exp	40	79						
n-butane	m/e	27	41	42	43	58			
	lit	23	26	13	100	17			
	exp	70	51	38	100	20			
1,3-butadiene	m/e	39	50	51	52	53	54		
	lit	91	24	23	11	66	100		
	exp	100	43	29	43	57	100		
ethylacetylene	m/e	37	38	39	50				
	lit	9	15	76	22				
	exp	32	36	76	40				
diacetylene	m/e	24	25	36	37	48	49	50	51
	lit	3	9	4	6	10	43	100	45
	exp	2	5	3	4	10	40	100	41
vinylacetylene	m/e	25	26	37	48	51	52	53	
	lit	4	11	5	3	50	100	4	
	exp	5	23	5	16	52	100	14	

Methane and butene were identified by comparing the retention times for these products on the gas chromatogram with those of injected samples of the pure compounds. Cis-, trans-, and 1-butene were not resolved.

Appendix 2: Data for Irradiation Experiments

Nonbreakdown, P(26) line

Experiment #	Pressure (torr)	# of pulses	Product yields (μmoles)					
			CH_4	C_2H_6	C_3H_8	C_2H_2	C_3H_6	C_4H_{10}
342	2	5000	.0022	.009	.019	.061	.0017	.014
376	2	5000	.0074	.020	.030	.160	.0021	.022
387	2	5000	.0045	.010	.019	.117	.0013	.019
396	4	4000	.0070	.041	.055	.570	.0018	.031
400	4	3070	.0064	.040	.057	.515	.0019	.029
403	4	2133	.0052	.030	.042	.379	.0013	.020
405	4	1090	.0039	.015	.015	.167	.0007	.009
334	5	1000	.0056	.026	.027	.195	.0033	.009

Nonbreakdown, P(14) line

Experiment #	Pressure	# of pulses	Products yields (peak area ÷ carbon #)			
			C_2H_6	C_3H_8	C_2H_2	$C_3H_6 + C_4H_{10}$
626	1	8917	8.63	7.35	25.7	6.46
579	2	7363	6.98	5.71	31.9	4.11
624	4	259	2.71	0.72	10.2	0.37
621	4	500	3.21	2.99	18.8	0.76
618	4	1000	4.34	2.75	29.8	1.08
607	4	2036	1.48	0.49	6.24	0.40

Breakdown, phenylisocyanate on porasil column

Experiment #	Pressure	# of pulses	Product yields (μmoles)					
			CH_4	C_2H_6	C_3H_8	C_2H_2	C_3H_6	C_4H_{10}
346	10	9	.040	.035	.028	2.01	.013	.008
375	5	1500	.40	.095	.034	22.0	.075	.003
383	20	20	.079	.041	.029	4.24	.016	.009
391	20	25	.091	.046	.033	4.36	.021	.011

Breakdown, n-octane on porasil column

Experiment #	Pressure	# of pulses	Product yields (μmoles)				
			C_2H_6	C_2H_2	C_3H_8	C_4H_{10}	C_4H_2
468	20	20	.085	6.07	-	-	.24
489	20	20	.119	10.2	.0039	.016	.29
493	10	40	.178	12.4	.029	.039	.75
495	10	20	.077	5.67	.012	.025	.26
500	10	10	.050	2.33	.0011	.011	.098

Breakdown, n-octane on porasil column, 10 torr ethylene, relative product yields with butadiene set = 1.00

Experiment #	511	517	520	521	523
# of pulses	30	35	30	30	150
ethane	2.07	2.59	0.31	0.15	0.93
acetylene	137	166	260	77	472
propylene	0.26	0.34	0.24	0.46	0.74
methylacetylene	0.70	0.13	0.15	0.23	0.58
butane	0.48	0.54	0.59	0.53	0.52
butenes	0.03	0.09	0.18	0.15	0.19
1,3-butadiene	1.00	1.00	1.00	1.00	1.00
ethylacetylene	-	-	0.13	0.08	0.98
diacetylene	4.85	11.8	21.1	17	48
vinylacetylene	0.36	0.72	0.84	0.91	1.71

Hydrogen Yields, nonbreakdown, 4 torr pure C_2H_4

Experiment #	# of pulses	H_2 (μmoles)
624	259	1.21
621	500	0.59
618	1000	0.46
615	1037	0.32
607	2036	0.21

Hydrogen Yields, nonbreakdown, 1:1 C_2H_4-C_2D_4 mixtures

Experiment #	Pressure	# of pulses	Product yield (μmoles)		
			H_2	HD	D_2
650	4	1000	.11	.03	.03
634	4	2000	.34	.20	.09
630	4	3000	.62	.47	.25
656	3	2000	.11	-	-
657	3	4000	.19	.04	-
660	3	8175	.59	.07	-
651	2	5000	.13	-	-
653	2	10000	.30	-	-